ACSNANO

www.acsnano.org

ARTICLE

Complete Restoration of Hearing Loss and Cochlear Synaptopathy via Minimally Invasive, Single-Dose, and Controllable Middle Ear Delivery of Brain-Derived Neurotrophic Factor–Poly(DL-lactic acid-*co*-glycolic acid)-Loaded Hydrogel

Qianru Yu,▽ Shengnan Liu,▽ Rui Guo,▽ Kuntao Chen, Yang Li, Dan Jiang, Shusheng Gong, Lan Yin,* and Ke Liu*

Cite This: https://doi.org/10.1021/acsnano.3c11049

Read Online

ACCESS | Metrics & More | Article Recommendations | Supporting Information

ABSTRACT: Noise-induced hearing loss (NIHL) often accompanies cochlear synaptopathy, which can be potentially reversed to restore hearing. However, there has been little success in achieving complete recovery of sensorineural deafness using nearly noninvasive middle ear drug delivery before. Here, we present a study demonstrating the efficacy of a middle ear delivery system employing brain-derived neurotrophic factor (BDNF)–poly-(DL-lactic acid-*co*-glycolic acid) (PLGA)-loaded hydrogel in reversing synaptopathy and restoring hearing function in a mouse model with NIHL. The mouse model achieved using the single noise exposure (NE, 115 dBL, 4 h) exhibited an average 20 dBL elevation of hearing thresholds with intact cochlear hair cells but a loss of ribbon synapses as the primary cause of hearing impairment. We developed a BDNF-PLGA-loaded thermosensitive hydrogel, which was administered via a single controllable injection into the tympanic cavity of noise-exposed mice, allowing its presence in the middle ear for a duration of 2 weeks. This intervention resulted in complete restoration of NIHL at frequencies of click, 4, 8, 16, and 32 kHz. Moreover, the cochlear ribbon synapses exhibited significant recovery, whereas other cochlear components (hair cells and auditory nerves) remained unchanged. Additionally, the cochlea of NE treated mice revealed activation of tropomyosin receptor kinase B (TRKB) signaling upon exposure to BDNF. These findings demonstrate a controllable and minimally invasive therapeutic approach that utilizes a BDNF-PLGA-loaded hydrogel to restore NIHL by specifically repairing cochlear synaptopathy. This tailored middle ear delivery system holds great promise for achieving ideal clinical outcomes in the treatment of NIHL and cochlear synaptopathy.

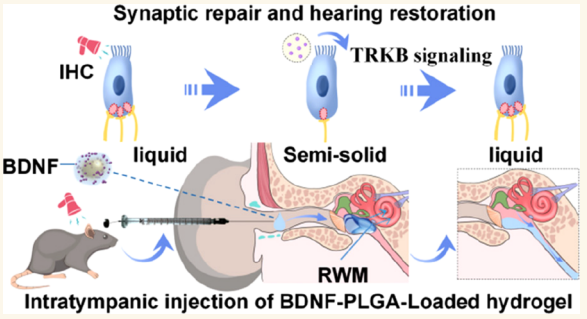

KEYWORDS: *noise-induced hearing loss, cochlear synaptopathy, brain-derived neurotrophic factor, BDNF-PLGA-loaded thermosensitive hydrogel, single injection, middle ear delivery system*

INTRODUCTION

Noise-induced hearing loss (NIHL) and cochlear synaptopathy are global health concerns, affecting hundreds of millions of individuals worldwide.[1] High-intensity and long-duration noise exposure can lead to significant loss of both cochlear hair cells, which are the primary sound sensory cells, and ribbon synapses, the sole type of afferent synaptic connections in the mammalian cochlea.[2−4] Conversely, moderate- and short-duration noise stimuli primarily cause damage to ribbon

Received: November 8, 2023
Revised: February 1, 2024
Accepted: February 5, 2024

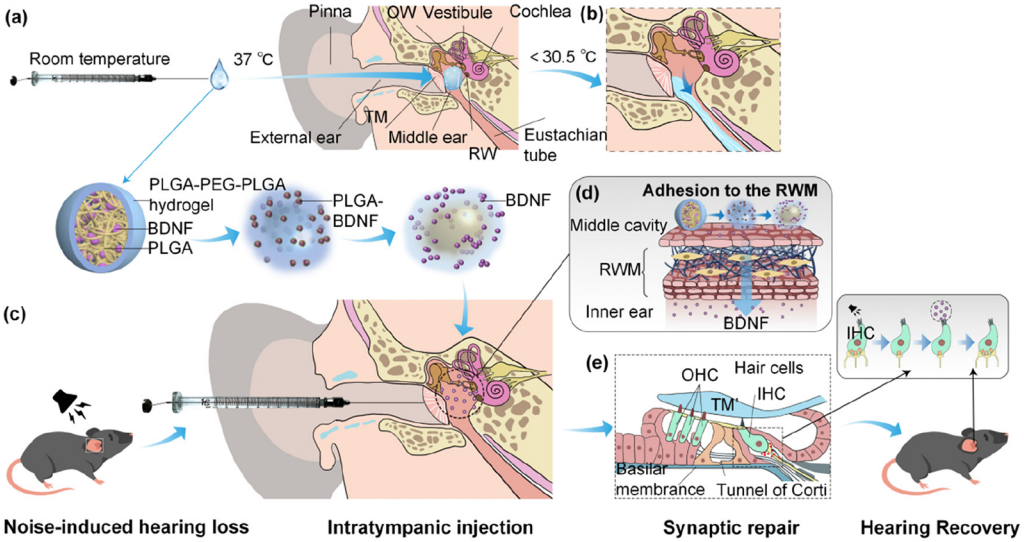

Figure 1. Schematic diagram of intratympanic injection of the temperature-sensitive type hydrogel-loaded BDNF-PLGA for the treatment of NIHL and cochlear synaptopathy. (a) PLGA-PEG-PLGA hydrogel-loaded PLGA-BDNF was injected into the middle ear in liquid state at room temperature (approximately 25 °C) and changed to be a semisolid state at the mouse body temperature (37 °C). (b) After the treatment, the semisolid hydrogel first switched to be a liquid state via reduction of the mouse body temperature (<30.5 °C), and finally the semisolid hydrogel completely passed out of the body through the eustachian tube. (c) Injection of the BDNF-PLGA-loaded thermosensitive hydrogel into middle ear restores NIHL via specific repair of cochlear synaptopathy. (d and e) The sol−gel−sol transition of PLGA-PEG-PLGA built stable contacts between the drug delivery system and RWM, and sustained release of the BDNF into inner ear can repair ribbon synaptic loss. TM, tympanic membrane. OW, oval window. RW, round window. RWM, round window membrane. OHC, outer hair cell. IHC, inner hair cell. TM′, tectorial membrane.

synapses without significantly impairing cochlear hair cells, resulting in a distinct type of hearing disorder known as noise-induced cochlear synaptopathy that is characterized by deficits in sound perception and language recognition. This form of peripheral hearing loss has also been referred to as "noise-induced hidden hearing loss".[3,5,6] Originally, cochlear synaptopathy was defined as a ribbon synaptic loss with no or only a transient-hearing threshold shifts in response to NE.[7−9] However, recent advances found that NIHL can be induced by cochlear ribbon synaptic damages alone whereas other cochlear components, such as cochlear hair cells and auditory nerves, remain normal, improving our understanding of cochlear synaptopathy compared with what it used to be.[10−12]

Currently, limited therapeutic approaches are available for the treatment of NIHL and cochlear synaptopathy.[13−15] While hearing aids and cochlear implants have proven beneficial for individuals with hearing impairment,[16,17] they are not ideal medical options for patients with NIHL due to inherent limitations. Hearing aids often reduce sound coding capacity, while cochlear implants require invasive surgical procedures.[18,19] Therefore, a pharmaceutical-based therapy that effectively restores NIHL holds great promise as the most anticipated approach for treatment. Two key factors significantly influence the outcome of sensorineural hearing loss treatment: the selection of drugs and the delivery system employed. Numerous drug candidates have demonstrated success in treating NIHL and cochlear synaptopathy.[20,21] Notably, brain-derived neurotrophic factor (BDNF) has been shown to provide complete protection to cochlear ribbon synapses from acoustic trauma by activating tropomyosin receptor kinase B (TRKB) signaling.[22−24] However, the choice of the drug delivery route is more crucial and often poses a challenge. The presence of the blood−labyrinth barrier (BLB) in the mammalian cochlea creates an anatomical barrier that restricts the entry of therapeutic substances into the inner ear, safeguarding the cochlea from external influences.[25,26] However, the BLB also hinders the delivery of therapeutic substances at sufficiently high concentrations via intravenous, intramuscular, subcutaneous, or oral administration.[27,28] Consequently, to minimize the limitations of BLB, there has been increasing interest in the development of optimized delivery systems that are middle-ear-based, highly efficient, minimally invasive, easily controlled, and fully biodegradable.[29,30]

An essential factor influencing the effective drug concentration within the inner ear is the contact situation of the delivery system with the round window membrane (RWM), including extended residence time and excellent compliance with the inner ear.[31] Recently, the use of biodegradable hydrogels as a continuous drug delivery system to the inner ear has emerged as a promising alternative to multiple injections, offering a longer residence time, reduced risk of infection associated with repeated injections, and prolonged drug effects.[29,32−34] To avoid secondary conductive hearing loss resulting from the application of hydrogels in the middle ear,[3,33] an ideal middle ear hydrogel should be thermosensitive, allowing it to transition between liquid and semisolid states. The liquid form facilitates injectability into the middle ear and subsequent expulsion via the eustachian tube, while the semisolid form enables prolonged retention in the middle ear, providing sustained drug release.[35,36] Poly(DL-lactic acid-*co*-glycolic acid) (PLGA)−polyethylene glycol (PEG)−PLGA (PLGA-PEG-PLGA), a extensively investigated thermally reversible hydrogel,[37,38] offers several advantages such as biodegradability, water solubility, slow-release properties, rapid gel-forming time, and minimal toxicity.[39,40] Meanwhile, the biodegradable polymer PLGA has been reported as an ideal carrier for preparing microspheres to achieve controllable drug

https://doi.org/10.1021/acsnano.3c11049
ACS Nano XXXX, XXX, XXX−XXX

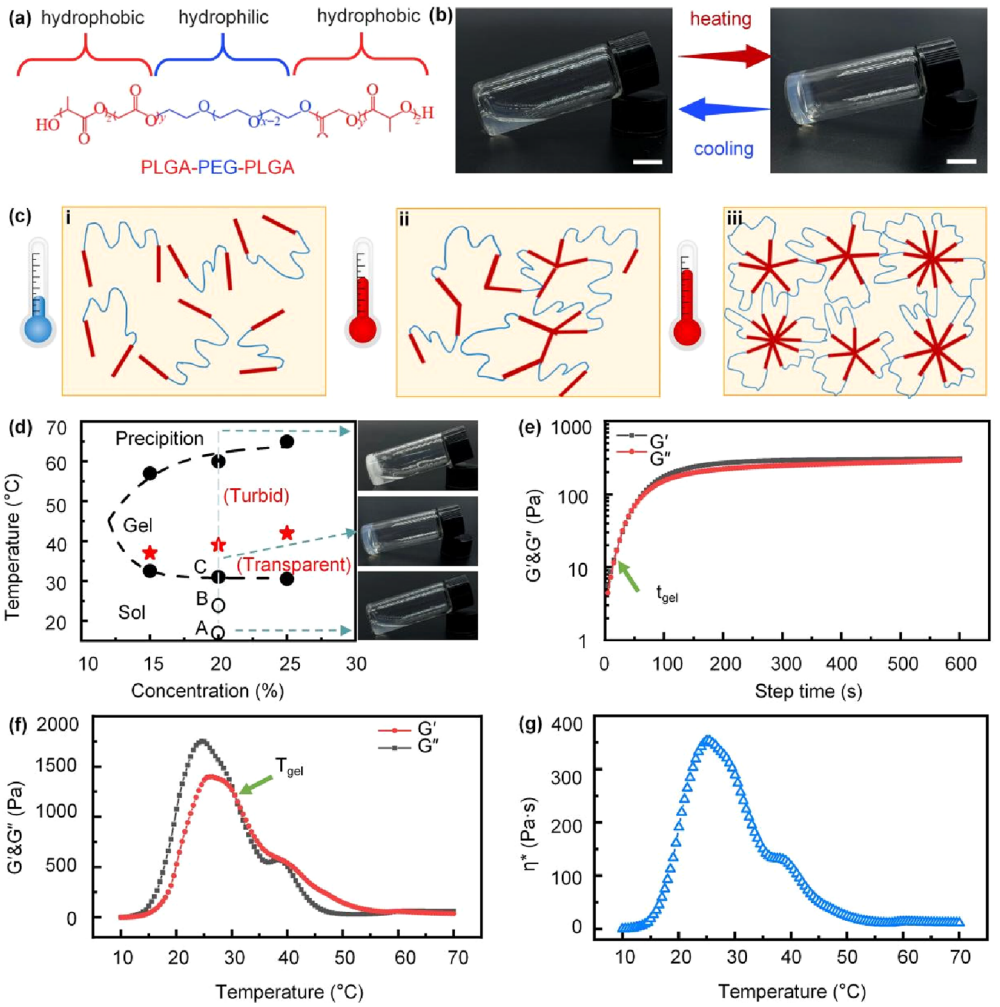

Figure 2. Thermally reversible hydrogel-loaded BDNF-PLGA for the treatment of NIHL and cochlear synaptopathy. (a) Synthesis route to the PLGA-PEG-PLGA triblock copolymer. (b) Sol−gel transition of PLGA-PEG-PLGA (20%, w/w). Scale bar represents 1 cm. (c) Mechanism of the PLGA-PEG-PLGA three-block micellar gelation process during thermal conversion. (d) Phase diagrams of PLGA-PEG-PLGA (20%, w/w) obtained from the vial inversion method. (e) Storage modulus (G') and loss modulus (G'') of the copolymer 20% (w/w) aqueous solution as a function of time at 37 °C. Dynamic viscoelastic analysis of PLGA-PEG-PLGA (20%, w/w). (f) Storage modulus (G') and loss modulus (G''). (g) Viscosity (η^*) of the aqueous mixture as a function of temperature.

delivery. The use of PLGA microspheres is crucial for maintaining the activities of proteins or peptides, allowing a single intratympanic injection of the P-G hydrogel to exhibit sustained release.[41,42]

In this study, we present a therapeutic approach using a tailored delivery system comprising a PLGA-PEG-PLGA thermosensitive hydrogel loaded with BDNF-PLGA. The aim is to treat NIHL and cochlear synaptopathy through targeted intratympanic injection. The thermal-sensitive PLGA-PEG-PLGA hydrogel-loaded BDNF-PLGA microspheres are designed to provide controlled and double sustained release of a therapeutic concentration of BDNF that can reach the inner ear via RWM. Following a single intratympanic injection, significant recovery from both NIHL and cochlear synaptopathy was observed, the treatment exhibited minimal side effects, and no residual hydrogel was detected in the middle ear. Thus, our study proposes an ideal and practical therapeutic strategy for addressing noise-induced deafness through the targeted repair of cochlear synaptopathy.

RESULTS AND DISCUSSION

Aschematic Visualization of Middle Ear Delivery of BDNF-PLGA-Loaded Hydrogel. In this study, we successfully developed a temperature-sensitive hydrogel loaded with BDNF-PLGA-PEG-PLGA, specifically designed for delivery of the middle ear into the inner ear. Our findings demonstrated that a single tympanic injection of this hydrogel led to the complete restoration hearing threshold in the NIHL mice model, which was achieved through the repair of cochlear ribbon synaptic damage. We also demonstrated that the hydrogel can be fully excreted from the middle ear cleft, and it does not impose any detrimental effects on the middle ear or tympanic membrane.

To provide a comprehensive understanding of the experimental procedure, we have created a schematic diagram illustrating the process involved in generating NIHL and cochlear synaptopathy, as well as the middle ear injection of a temperature-sensitive hydrogel loaded with BDNF-PLGA. The hydrogel, exhibiting thermosensitivity, was administered in its liquid state at room temperature (approximately 25 °C), and when subjected to body temperature (37 °C) it underwent a

https://doi.org/10.1021/acsnano.3c11049
ACS Nano XXXX, XXX, XXX−XXX

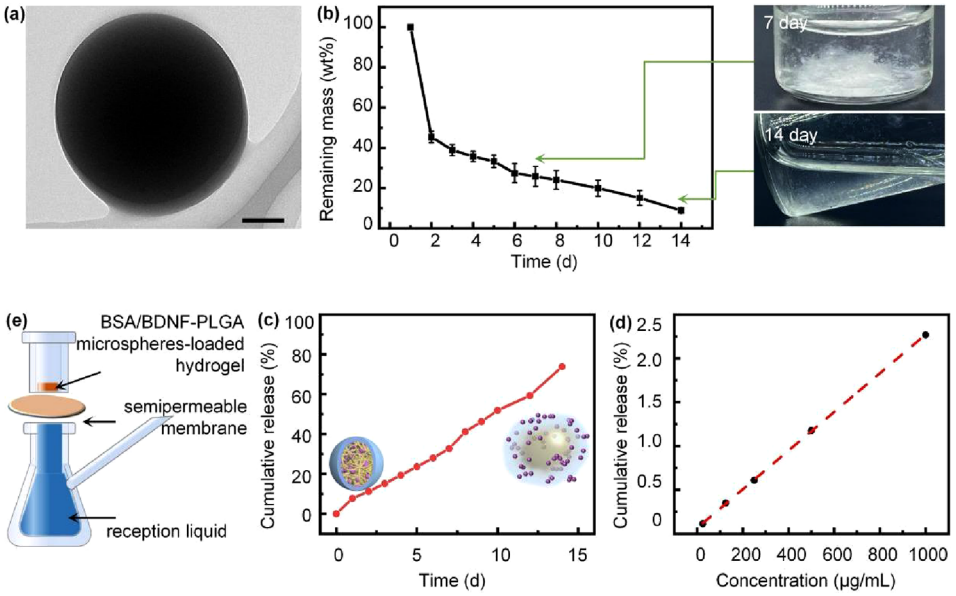

Figure 3. Slow release performance of PLGA-PEG-PLGA hydrogels as drug delivery systems. (a) TEM image of BDNF-PLGA microspheres. Scale bar represents 100 nm. (b) Remaining mass ratio of in situ hydrogel-loaded BDNF-PLGA microspheres in PBS at 37 °C over time. Insets show photographs of the degradation of hydrogel-loaded BDNF-PLGA microspheres in PBS at various stages at 37 °C. (c) Cumulative release of the PLGA-PEG-PLGA hydrogel with BSA loaded in PLGA microspheres. (d) Standard curves of BSA. (e) A customized diffusion cell system to simulate in vitro skin permeation.

phase transition to a semisolid state (Figure 1a). This transformed hydrogel allowed for prolonged retention in the middle ear. The schematic diagram (Figure 1b) depicts the eustachian tube serving as the anatomical excretory pathway for the middle ear contents. Following treatment, when the temperature of the middle ear decreased to below 30.5 °C, the hydrogel reverted to its liquid state, facilitating its expulsion through the eustachian tube. By injecting the temperature-sensitive hydrogel loaded with BDNF-PLGA into the middle ear, complete restoration of NIHL was achieved through the repair of cochlear synaptopathy after noise exposure in mice (Figure 1c–e).

Thermoreversible PLGA-PEG-PLGA Hydrogel Exhibits a Sol–Gel Conversion and Gelation Mechanism. To elucidate the thermoreversible behavior of the PLGA-PEG-PLGA hydrogel, the sol–gel conversion process and phase diagram associated with its gelation mechanism were extensively studied. The composition of the hydrogel, comprising hydrophobic PLGA and hydrophilic PEG, is depicted in Figure 2a. This thermoreversible property enables the PLGA-PEG-PLGA hydrogel to exist in a liquid state at room temperature, facilitating its suitability for middle ear injection. Following injection, the hydrogel undergoes a phase transition, transforming into a gel state upon reaching body temperature (Figure 2b). The micellar gelation scheme for the PLGA-PEG-PLGA triblock copolymer is presented in Figure 2c. A representative phase diagram (Figure 2d) demonstrates the sol–gel transition property and explores the impact of concentration on the gel transition temperature. The sol–gel and critical gelation temperatures (CGTs) near body temperature are crucial for inner ear administration. At lower temperatures, the hydrophobic interactions become prominent, leading to the formation of micelles or micellar groups consisting of a PLGA core and a PEG shell, both fully dispersed in water (Figure 2c(i,ii)), corresponding to points a and b in Figure 2d. As the temperature rises to 31 °C (point C in Figure 2d), these micelles aggregate through hydrophobic interactions mediated by PLGA, resulting in the formation of a three-dimensional network structure and achieving a sol–gel transition (Figure 2c(iii)). With an increase in the polymer mass fraction from 15% to 25%, the sol–gel phase transition temperature gradually decreases while the gel-precipitation phase transition temperature increases. The turbidity observed in the gel is attributed to the enhanced aggregation and accumulation of interactions between micelles. When the temperature approaches 60 °C, the hydrophobic PLGA chains in micelles undergo significant shrinkage and the hydrophilic PEG chains become dehydrated, leading to the precipitation of overagglomerated micelles in water.[43] To ensure the stability of in situ drug release from PLGA-PEG-PLGA, the modulus of hydrogels was measured at 37 °C to evaluate their rapid gelation time and viscoelastic changes at body temperature (Figure 2e). Below the CGT, the PLGA-PEG-PLGA solution exhibits liquid-like behavior, indicated by $G'' > G'$. However, upon incubation at 37 °C, G' rapidly increases, surpassing G''. The gelation time is defined as the point where $G' = G''$on the modulus curve as a function of time. The modulus and viscosity (η) of the 20% copolymer mixture were monitored as a function of temperature (Figure 2f and g). Initially, $G'' > G'$ and both $G'$and G''were relatively low, signifying that PLGA-PEG-PLGA exists in a free-flowing sol state. As the temperature increases, G' exhibits a rapid increase. The sol–gel transition temperature is determined to be approximately 30.5 °C at the point where $G' = G''$. Further temperature increases to 40 °C and above result in the precipitation of the polymer, leading to a decrease in gel strength. The complex viscosity η^* exhibits a similar trend with respect to temperature.

The investigation of the PLGA-PEG-PLGA hydrogel reveals its distinctive thermoreversible properties, including sol–gel conversion and the gelation mechanism. The sol–gel transition temperature close to body temperature and the swift gelation

https://doi.org/10.1021/acsnano.3c11049
ACS Nano XXXX, XXX, XXX–XXX

time at 37 °C highlight the potential of this hydrogel for controlled drug release in situ.

Sustained Release Performance of Drug Delivery Systems: Morphology and Degradation. The drug delivery systems' sustained release performance was evaluated through various analyses. Transmission electron microscopy (TEM) images revealed the desirable spherical morphology of the BDNF-PLGA microspheres, exhibiting a smooth surface (Figure 3a). The degradable behavior of PLGA-PEG-PLGA loaded with BDNF-PLGA was investigated at different time points in phosphate-buffered saline (PBS) at 37 °C. The results demonstrated that PLGA-PEG-PLGA loaded with BDNF-PLGA underwent complete degradation within a span of two weeks (Figure 3b). To examine the controlled drug release in the delivery systems, bovine serum albumin (BSA) was utilized as a surrogate for BDNF. In vitro drug release (BSA/BDNF) was assessed using a customized diffusion cell system that simulated in vitro skin permeation (Figure 3e). The release of BSA/BDNF occurred through a combination of diffusion, degradation, and erosion of the PLGA microspheres, as well as degradation of the hydrogel carriers. The cumulative release of the drug (BSA/BDNF) in PBS was plotted (Figure 3c) and quantified using the Micro BCA method, generating a standard curve (Figure 3d). The results demonstrated a stable, effective, highly loaded, and long-term release rate system.

Overall, the drug delivery systems exhibited a promising sustained release performance. The TEM images confirmed the favorable morphology of BDNF-PLGA microspheres, while the degradation studies revealed the complete degradation of PLGA-PEG-PLGA loaded with BDNF-PLGA within a two-week period. The in vitro drug release experiments utilizing BSA as a model drug demonstrated a controlled release through various mechanisms. These findings highlight the potential of drug delivery systems for stable and efficient sustained drug release.

To achieve minimally invasive delivery of target drugs into the inner ear, various hydrogel materials have been previously studied for tympanic injection into the middle ear.[29,31,44,45] These hydrogels transition from an injectable sol state to a gel state, serving as reservoirs for sustained release drugs. The gelation schemes commonly involve click-cross-linking or photocuring. However, these chemically formed drug delivery carriers often consist of large and hard materials, potentially leading to long-term conductive hearing loss.[29,46] Additionally, a termination mechanism (e.g., the discharge of the drug and vector through the eustachian tube) should be in place to address drug toxicity or other potential detrimental effects on the middle/inner ear faction that may occur during sustained release. The process of chemical cross-linking to form gels is typically irreversible or involves the use of specific enzymes. In contrast, the PLGA-PEG-PLGA hydrogel possesses a thermo-sensitive characteristic, enabling it to transition from a liquid to a semisolid state.[33,34] This property offers a strategy for middle ear sustained-release drug delivery in the treatment of sensorineural deafness without inducing conductive hearing loss.

In our study, PLGA-PEG-PLGA served as an ideal middle ear hydrogel, and we precisely selected the temperature-sensitive hydrogel concentration so that it could be injected into the middle ear in the form of a liquid and converted into a semisolid state to stick firmly to the RWM to slowly release drugs.[47,48] Based on these results, we further studied the corresponding correlations among the PLGA-PEG-PLGA concentration, transition state, and mechanism according to the application scenario. Our design package for the entire delivery system included temperature-sensitive gels, slow-release microspheres, BDNF, and a middle ear injection. We believe that the value of the whole system is mainly due to the twofold slow release of BDNF through the PLGA microspheres and hydrogels; that is, the release of BDNF occurs through a combination of diffusion, degradation, and erosion of the PLGA microspheres, as well as degradation of the hydrogel carriers. The property of transformation into a semisolid at body temperature after injection in a liquid form and stable adhesion to the RWM is the key reason for choosing the PLGA-PEG-PLGA hydrogel as a delivery carrier, which involves two steps of degradation: (1) the gradual hydrolysis of the semisolid hydrogel at body temperature and (2) the liquid phase transformation, which is triggered by a slightly lower temperature, causes the liquid state of the hydrogel to flow out via the eustachian tube and finally achieves zero residue of the hydrogel in the middle ear.

Biocompatible Evaluation of the PLGA-PEG-PLGA Hydrogel. The biocompatibility of the PLGA-PEG-PLGA hydrogel was assessed through in vitro and in vivo experiments. In the in vitro study, cochlear basilar membrane cultures were established to observe the cochlear hair cells and synapses, with a specific focus on minimizing spatial distribution effects (Figure S1a). Hair cell counts were performed, and in the control group the average number of outer hair cells (OHCs) was 35.25 ± 0.98, while the average number of inner hair cells (IHCs) was 11.00 ± 0.27 (Figure S1b and d). Synaptic spot counts were also conducted in each IHC, revealing a mean number of 22.05 synaptic spots (Figure S1c and e). Subsequently, cochlear explants were subjected to DMEM/F12 medium containing the PLGA-PEG-PLGA hydrogel. The average number of the OHCs was 35.13 ± 0.93, the average number of the IHCs was 11.13 ± 0.30 (Figure S1b and d), and the mean number of synaptic puncta was 21.56 ± 0.46 (Figure S1c and e). No significant differences were observed between the tested and control groups ($P > 0.05$), indicating the excellent biocompatibility of the PLGA-PEG-PLGA hydrogel. To further evaluate the safety of the PLGA hydrogel in vivo, we investigated possible changes in auditory brainstem response (ABR) thresholds in mice at days 7 and 14 following tympanic injection of the hydrogel (Figure S2a). Notably, no significant differences were observed between the control and experimental groups at click and the frequencies of 4, 8, 16, and 32 kHz, respectively ($P > 0.05$, Figure S2b and c). These findings suggest that tympanic injection of the PLGA-PEG-PLGA hydrogel does not impair the hearing capacity of the mice. Previous studies have demonstrated the biocompatibility and slow-release properties of PLGA-PEG-PLGA.[36] Our investigation also confirmed the safety of P-G hydrogels after intratympanic injection.

Therapeutic effects of BDNF on NIHL and Cochlear Synaptopathy In Vitro. In addition to its biocompatibility, the therapeutic effects of BDNF on NIHL and cochlear synaptopathy were investigated in vitro. Cochlear basilar membrane cultures were treated with an NK (*N*-methyl-D-aspartate and kainate) solution to simulate noise-induced excitotoxicity (Figure S3a).[49,50] The mean number of synaptic spots was 18.40 ± 0.53 in the NK-treated group, whereas the mean number of synaptic puncta in the control group was 22.47 ± 0.67, revealing a significant difference ($P < 0.0001$). Importantly, the group treated with NK + BDNF showed a

https://doi.org/10.1021/acsnano.3c11049
ACS Nano XXXX, XXX, XXX−XXX

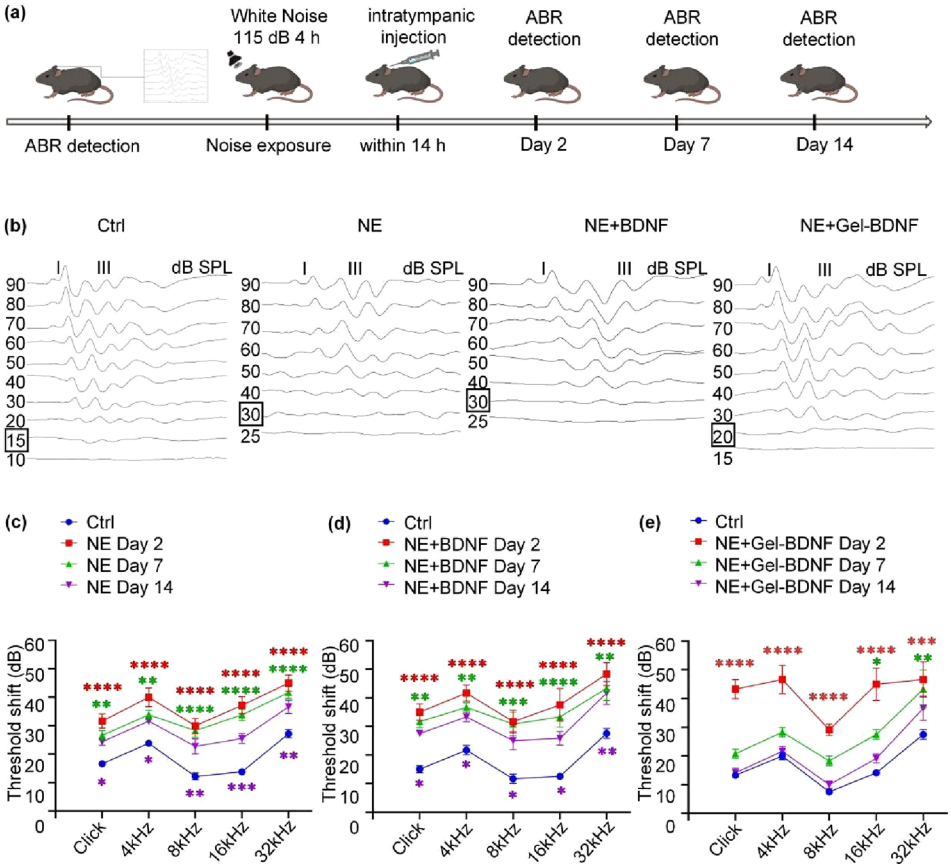

Figure 4. Intratympanic injection of temperature-sensitive hydrogel-loaded BDNF-PLGA significantly decreases the ABR threshold in the noise-induced deaf mice. (a) Schematic diagram of the experimental procedure in this study. (b) Representative waveforms of the ABR detection in each group on day 14 after NE. The sound intensity decreases in every 5−10 dB SPL from the initial 90 dB SPL, and the black solid frame indicates the ABR threshold. (c−e) Changes of ABR thresholds in the groups of NE (n = 9 animals, 9 ears), NE + BDNF (n = 6 animals, 6 ears), and NE + Gel-BDNF (n = 6 animals, 6 ears) on days 2, 7, and 14, respectively. ABR: auditory brainstem response. The red asterisks (*) represent the statistical significance among the groups of NE, NE + BDNF, and NE + Gel-BDNF on day 2 and ctrl. The green asterisks (*) represent the statistical significance among the groups of NE, NE + BDNF, and NE + Gel-BDNF on day 7 and ctrl. The purple asterisks (*) represent the statistical significance among the groups of NE, NE + BDNF, and NE + Gel-BDNF on day 14 and ctrl. P value: *p < 0.05, **p < 0.01, ***p < 0.001, ****p < 0.0001.

significant enhancement in the ribbon synaptic number (22.05 ± 0.37) compared to the NK group (P < 0.001), with no significant difference observed compared to the control group (P > 0.05) (Figure S3b,c). These results demonstrate that BDNF has the potential to repair damaged cochlear ribbon synapses in an in vitro model mimicking noise trauma.

Therapeutic Effects of BDNF on NIHL and Cochlear Synaptopathy in Mice. To further validate the therapeutic effects of BDNF on NIHL associated with the loss of cochlear ribbon synapses, we employed a mouse model exposed to noise (Figure S4a). BDNF solution was delivered to the inner ear through a surgical approach via a posterior semicircular canal. Hearing assessments were conducted on days 2, 7, and 14 postnoise exposure. And we found that the group receiving the BDNF injection via the semicircular canal (NE + BDNF′) exhibited a significant reduction in ABR thresholds across all tested frequencies on days 7 and 14 after injection, with no significant difference observed on day 14 compared to the control group (Figure S4b) and with significant statistical difference observed on day 14 compared to the NE group. These results demonstrate that the inner ear delivery of BDNF via a surgical procedure through the semicircular canal effectively treats NIHL in mice.

The amplitude and latency of ABR wave I have been reported to reflect the function of cochlear ribbon synapses.[3,51,52] Thus, we further examined the changes in the ABR wave I amplitude and latency in this study. The NE group exhibited significantly decreased amplitudes of ABR wave I at all tested frequencies compared to the control group. In contrast, the NE + BDNF′ group showed significantly increased amplitudes of ABR wave I across all tested frequencies compared to the NE group (Figure S4c). Similarly, significantly increased latency of ABR wave I was observed at each detected frequency in the NE group compared to that in the control group. In contrast, the NE + BDNF′ group exhibited significantly decreased latencies of ABR wave I across all frequencies compared to the NE group (Figure S4d). These findings indicate functional recovery of cochlear ribbon synapses, as there were no significant differences in ABR wave I amplitude or latency between the NE + BDNF′ and control groups.

To investigate whether BDNF could repair the noise-induced loss of cochlear ribbon synapses in mice, we conducted quantitative analysis of ribbon synapses. The ribbon presynaptic motif was labeled with anti-RIBEYE/CtBP2, while postsynaptic proteins were traced using anti-GluR2.[49,53,54]

https://doi.org/10.1021/acsnano.3c11049
ACS Nano XXXX, XXX, XXX−XXX

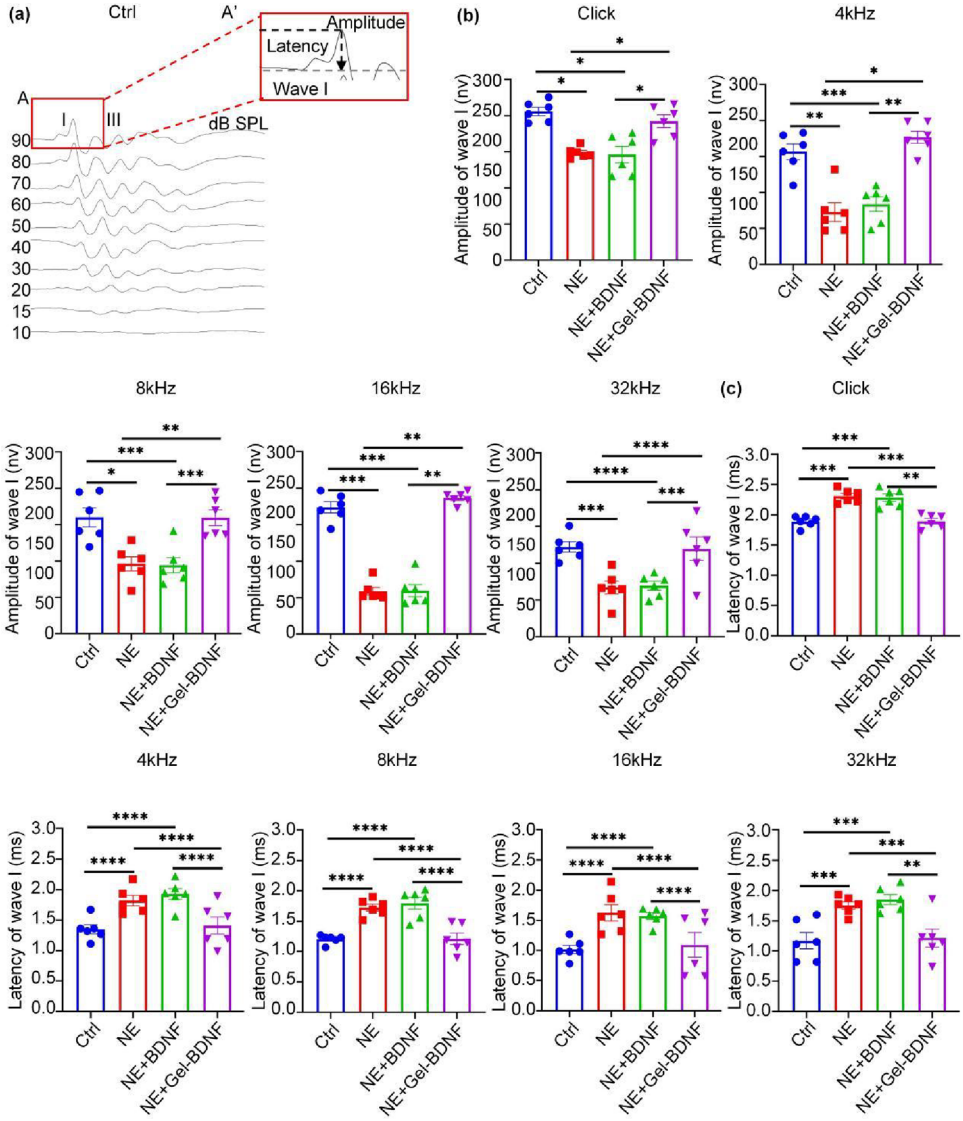

Figure 5. Intratympanic injection of temperature-sensitive hydrogel-loaded BDNF-PLGA significantly restores the amplitude and latency of ABR wave I in the noise-induced deaf mice. (a,A) Representative waveform of wave I amplitude and latency at the ctrl group on day 14 after NE; the red solid frame indicates ABR wave I. (a,A′) Enlarged image in upper right panel. (b and c) Changes in the ABR wave I amplitude and latency, respectively, in the ctrl, NE, NE + BDNF, and NE + Gel-BDNF groups on day 14 after NE. The highest amplitude and shortest latency of ABR wave I were seen at the group of NE + Gel-BDNF. P value: *$p < 0.05$, **$p < 0.01$, ***$p < 0.001$,**$p < 0.0001$ ($n = 6$ animals, 6 ears).**

Synaptic numbers were assessed on day 14 post-NE in the spatial apical, middle, and basal turns of the cochlea. In the control group, the numbers of merged signals comprising presynaptic and postsynaptic positive puncta were 10.67 ± 0.49 (apex), 10.88 ± 0.43 (middle), and 7.11 ± 0.18 (base). In the NE group, these numbers were 6.15 ± 0.26 (apex), 7.25 ± 0.24 (middle), and 3.92 ± 0.21 (base). Notably, the NE + BDNF′ group displayed numbers of 9.42 ± 0.38 (apex), 10.40 ± 0.22 (middle), and 6.77 ± 0.41 (base). The highest numbers of synaptic puncta were observed in the control and NE + BDNF′ groups, with no significant differences between the two (Figure S5a and b). Thus, these results demonstrate that inner ear delivery of BDNF through the surgical approach of the posterior semicircular canal can significantly repair noise-induced cochlear synaptopathy.

The therapeutic effects of BDNF on NIHL and cochlear synaptopathy were confirmed in the mouse model, highlighting the potential of BDNF as a promising treatment strategy. The delivery of BDNF through the posterior semicircular canal successfully restored auditory thresholds, improved ABR wave I characteristics, and promoted the recovery of cochlear ribbon synapses. These findings emphasize the therapeutic efficacy of BDNF in combating noise-induced hearing impairments and supporting the restoration of cochlear synaptic function.

Intratympanic Injection of BDNF-PLGA-Loaded Hydrogel Completely Restores NIHL. To assess the restorative potential of intratympanic injection of a temperature-sensitive hydrogel loaded with BDNF-PLGA, we employed mouse models with NIHL characterized by elevated ABR thresholds (Figure 4a–d). Our study demonstrated that intratympanic injection of hydrogel-loaded BDNF-PLGA significantly reduced ABR thresholds across frequencies on days 7 and 14 postinjection. Notably, no significant difference in ABR thresholds was observed on day 14 compared with the

https://doi.org/10.1021/acsnano.3c11049
ACS Nano XXXX, XXX, XXX−XXX

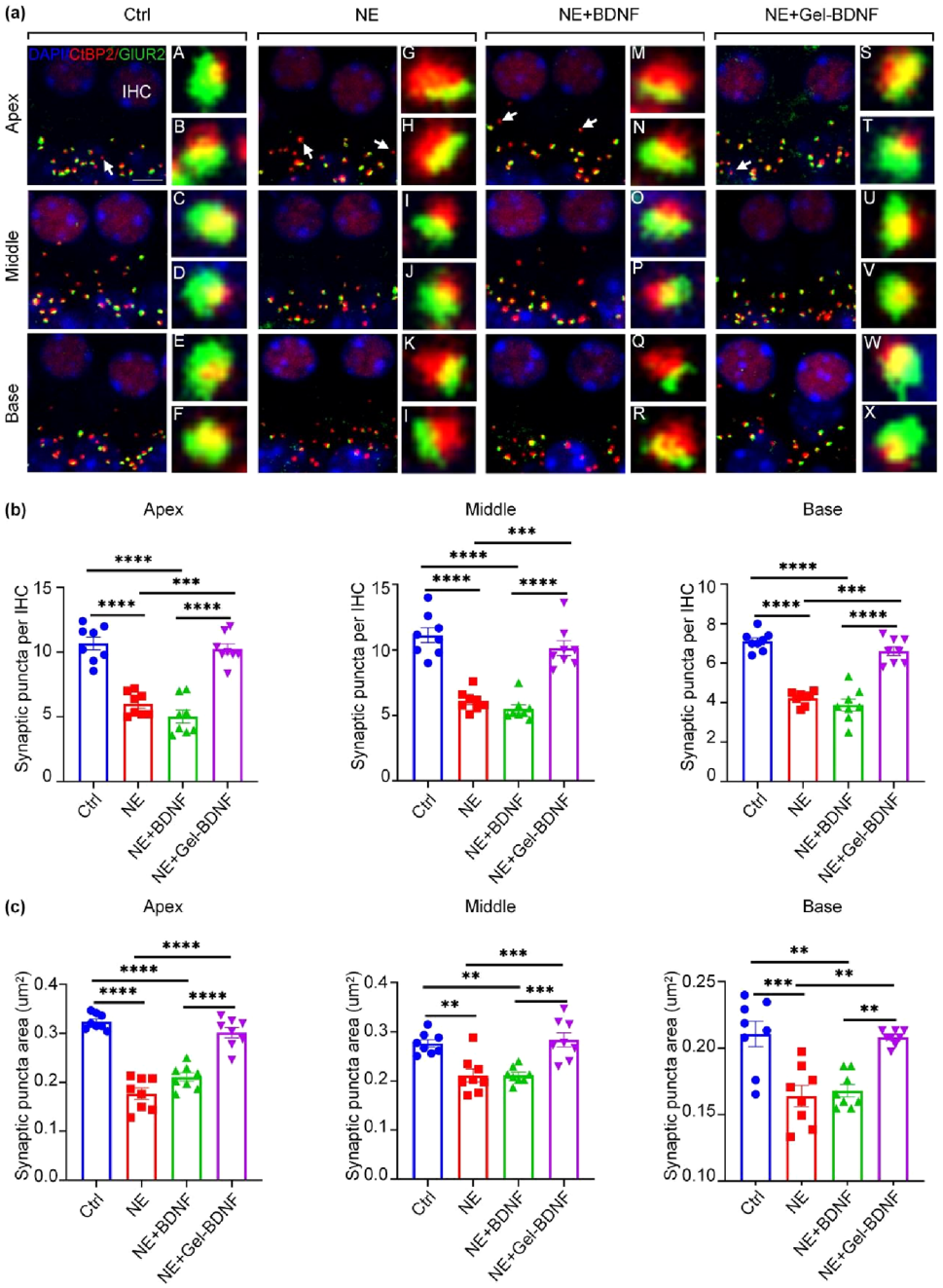

Figure 6. Intratympanic injection of thermally reversible hydrogel-loaded BDNF-PLGA significantly repair the noise-induced cochlear synaptopathy. (a) Presynaptic identification was accomplished by anti-CtBP2 (red), the postsynaptic motif was identified using anti-GluR2 (green), the merged synaptic puncta are shown in orange, and the nuclei of cochlear HCs were stained using DAPI (blue). A number of synaptic spots appeared at ctrl and NE + Gel-BDNF groups, and the lowest number of synaptic puncta were seen at the groups of NE and NE + BDNF. (a,A–X) Enlarged view of paired synaptic puncta. The white arrows indicate unpaired synapses. Scale bar represents 5 μm. (b) Quantitative analysis of changes in ribbon synaptic numbers across the frequencies in all the groups. (c) Quantitative analysis of the ribbon synaptic size across the frequencies in all the groups. P value: *$p < 0.05$, **$p < 0.01$, ***$p < 0.001$, ****$p < 0.0001$ ($n = 4$ animals, 4 ears).

control group (Figure 4e), indicating a complete restoration of ABR thresholds in the Gel + BDNF group relative to the controls. Furthermore, we analyzed the changes in ABR wave I amplitude and latency. The NE group exhibited a significant reduction in ABR wave I amplitude and an increase in latency compared to those of the control group (Figures 5a–c and S6). Similarly, the NE and NE + BDNF treatment groups displayed decreased amplitude and increased latency across frequencies. However, the NE + Gel-BDNF treatment group showed increased amplitude and shortened latency of ABR wave I compared to the control group.

These findings highlight the effectiveness of intratympanic injection of a temperature-sensitive hydrogel loaded with BDNF-PLGA in restoring NIHL in mice. The treatment led to a significant improvement in ABR thresholds, amplitudes, and latencies, indicating the successful recovery of auditory function. The use of the gel-based delivery system provides a promising therapeutic approach for the treatment of NIHL,

https://doi.org/10.1021/acsnano.3c11049
ACS Nano XXXX, XXX, XXX–XXX

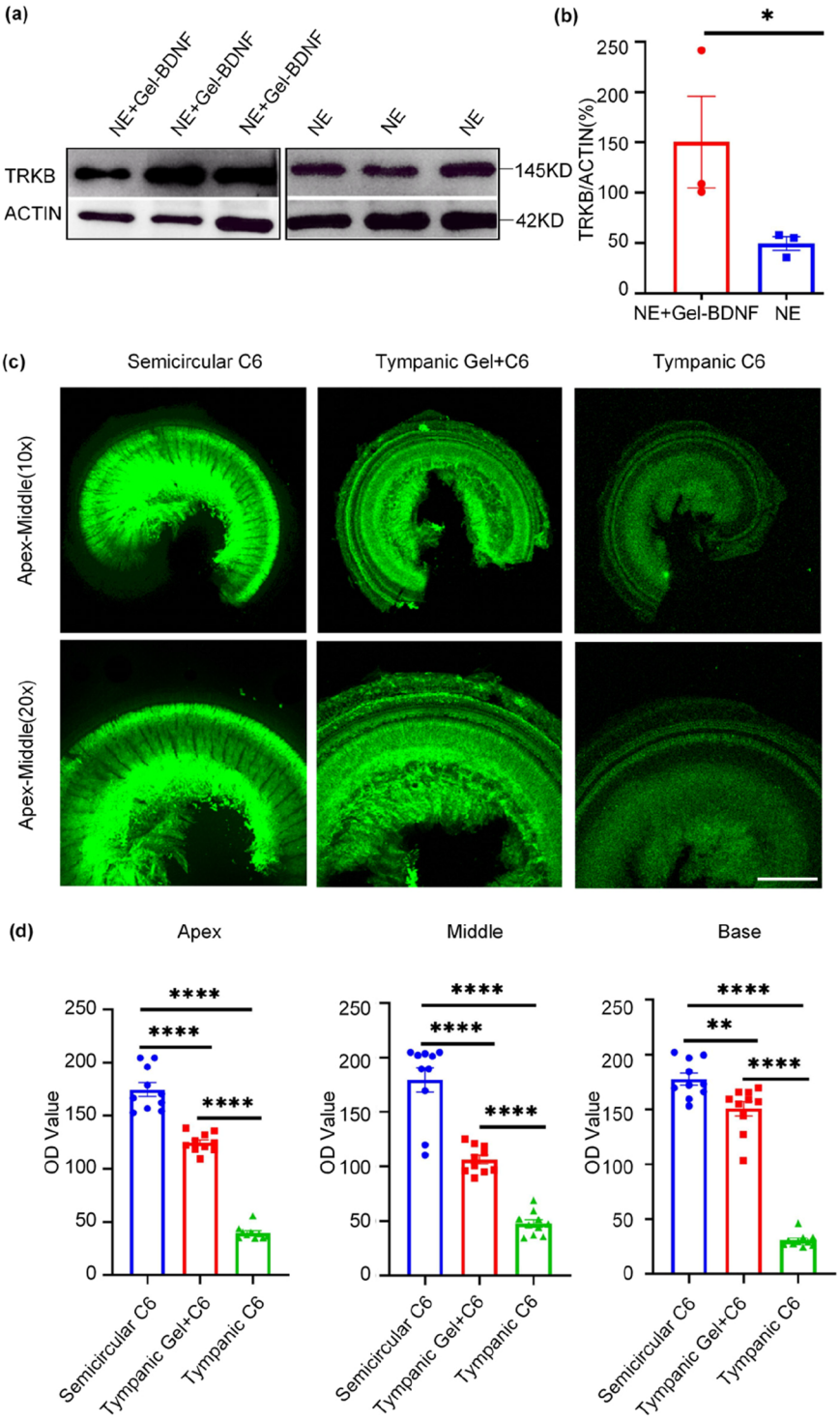

Figure 7. Sustained release of BDNF-PLGA-loaded hydrogel in the middle ear ensures the activation of TRKB singling and a high dose of green fluorescence-labeled C6 dye in the inner ear. (a and b) Compared with the NE group, significantly enhanced expression of TRKB was found on the day 2 after NE in the group of NE + Gel-BDNF. (c) Immunostaining revealed the changes of green fluorescence-labeled C6 dye on day 1 after injection of the hydrogel loaded with green fluorescence-labeled C6 dye, and increased intensity of fluorescence green fluorescence-labeled C6 dye can be found in the groups of tympanic Gel + C6 and semicircular C6. Scale bar represents 20 μm. (d) Quantitative analysis of fluorescence intensity in the three groups. P value: *$p = 0.0359$, **$p < 0.01$, ****$p < 0.0001$. ($n = 3$ animals, 3 ears).

offering the potential for clinical translation and enhanced patient outcomes.

Repair of Cochlear Synaptopathy through Intratympanic Injection of the BDNF-PLGA-Loaded hydrogel. Following the intratympanic injection of the BDNF-PLGA-loaded hydrogel, we conducted a quantitative analysis of ribbon synaptic spots on day 14 after NE treatment. Only the overlapped synaptic puncta, representing intact synapses with both pre- and postsynaptic signals, were included in the calculation. In the control group, the number of synaptic spots was 10.67 ± 0.49 (apex), 11.13 ± 0.58 (middle), and 7.11 ± 0.16 (base). In the NE group, the numbers decreased to 5.99 ±

https://doi.org/10.1021/acsnano.3c11049
ACS Nano XXXX, XXX, XXX−XXX

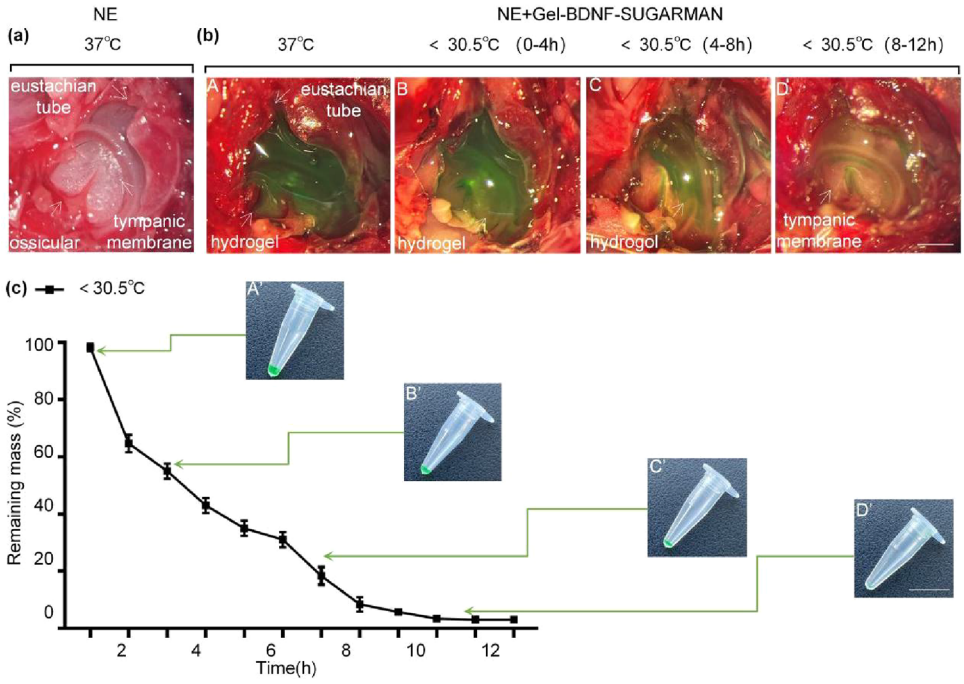

Figure 8. Middle ear delivery of the BDNF-PLGA-loaded hydrogel can be completely excreted through the eustachian tube. (a) The view of the tympanic chamber in normal adult mice before injection of the hydrogel. Scale bar represents 1 mm. (b,A−D) Dynamic tympanic images in response to the temperature changes and time durations after the intratympanic injection of hydrogel-loaded BDNF-PLGA microspheres dyed with SUGARMAN food coloring (fruit green). After intermittent ice application for 8−12 h (<30.5 °C), the hydrogel-loaded BDNF-PLGA microspheres (SUGARMAN) were completely metabolized through the eustachian tube. Scale bar represents 1 mm. (c) Variation of the remaining mass ratio of hydrogel-loaded BDNF-PLGA microspheres (SUGARMAN) in the middle ear (<30.5 °C) with time. (b,A′−D′) Degradative photographs of hydrogel-loaded BDNF-PLGA microspheres (SUGARMAN) in the middle ear at different stages (<30.5 °C). Scale bar represents 1 cm.

0.32 (apex), 6.12 ± 0.27 (middle), and 4.22 ± 0.12 (base). In the NE + BDNF group, the numbers changed to 5.03 ± 0.50 (apex), 5.50 ± 0.31 (middle), and 3.88 ± 0.30 (base). Notably, in the NE + Gel-BDNF group, the numbers significantly increased to 10.24 ± 0.41 (apex), 10.14 ± 0.57 (middle), and 6.61 ± 0.23 (base). The greatest number of synaptic puncta was observed in both the control and NE+Gel-BDNF groups, with no significant differences between them (Figure 6a and b). These findings highlight the complete restoration of noise-induced quantitative synaptic loss through 2 weeks-long application of BDNF-PLGA-loaded hydrogel in the middle ear of mice.

Furthermore, we analyzed the sizes of merged synaptic puncta using the Adobe Photoshop CS6 software. In the control group, the mean synaptic size was 0.32 ± 0.06 (apex), 0.28 ± 0.08 (middle), and 0.21 ± 0.09 (base). In the NE group, the mean size decreased to 0.18 ± 0.06 (apex), 0.21 ± 0.01 (middle), and 0.16 ± 0.08 (base). In the NE + BDNF group, the sizes were 0.21 ± 0.09 (apex), 0.21 ± 0.06 (middle), and 0.17 ± 0.04 (base). Notably, the NE + Gel-BDNF group exhibited increased sizes of 0.30 ± 0.01 (apex), 0.28 ± 0.01 (middle), and 0.21 ± 0.02 (base) (Figure 6a−c). Similar to the number of synaptic puncta, the largest synaptic spots were observed in the control and NE + Gel-BDNF groups with no significant difference between them. These results suggest that the sustained release of the BDNF-PLGA-loaded hydrogel can fully restore the size of synaptic puncta.

The application of the hydrogel leads to a significant increase in the number and size of intact synapses, indicating the successful restoration of synaptic connectivity. This finding highlights the potential clinical application of a BDNF-PLGA-loaded hydrogel as an effective treatment strategy for cochlear synaptopathy associated with noise exposure.

Analysis of Cochlear Hair Cells and Spiral Ganglion Cells. In this study, we investigated the changes in cochlear hair cells and spiral ganglion cells 14 days after NE. In the NE group, there was no significant loss of OHCs across the apical, middle, and basal turns compared to the control group. Similarly, no statistical significance was observed in the number of IHCs and OHCs among all of the groups (Figure S7). Additionally, we examined the postsynaptic auditory nerve fibers labeled with anti-NF200 on day 14 after NE, and no significant differences were found among the tested groups. These results suggest that NE causes cochlear synaptopathy without an apparent loss of the OHCs, IHCs, and spiral ganglion cell nerves (Figures S8 and S9).

Thus, our animal model successfully induced NIHL with cochlear synaptopathy, yet no apparent damage to cochlear hair cells or auditory nerves was observed.[55−57] This emphasizes the crucial role of repairing ribbon synapses in achieving complete recovery from hearing loss. However, the therapeutic outcomes observed in this study may not be directly applicable to animal models with significant loss of hair cells or auditory nerve. Here, it should be noted that the current understanding of cochlear synaptopathy is gradually being updated. As we have described previously, it not only refers to the situation of cochlear synaptic damage combined with no or transient shifting in the hearing thresholds, but may also involve cases of significant or long-lasting hearing loss induced by noise,[11,12] aging, ototoxic drugs,[10,58] and congenital factors.[59,60]

https://doi.org/10.1021/acsnano.3c11049
ACS Nano XXXX, XXX, XXX−XXX

Activation of the TRKB Signaling Pathway through Delivery of the BDNF-PLGA-Loaded Hydrogel. To assess the intratympanic delivery efficiency of in situ hydrogel-loaded BDNF-PLGA into the inner ear, we evaluated the activation of the TRKB signaling pathway in cochlear tissue through Western blot analysis. The expression of TRKB was significantly higher in the cochlear tissue after intratympanic injection of temperature-controlled in situ hydrogel-loaded BDNF-PLGA ($P < 0.05$, Figure 7a and b). This finding indicates that the hydrogel effectively delivers BDNF into the inner ear, subsequently leading to the activation of the downstream TRKB signaling pathway. Additionally, we utilized a thermosensitive in situ hydrogel loaded with green fluorescence labeled C6 dye.[61,62] Visualization of the hydrogel's penetration was conducted using immunofluorescence intensity analysis on day 1 after green fluorescence-labeled C6 dye administration in three different groups: tympanic C6 (green fluorescence-labeled C6 dye injection into the middle ear), semicircular C6 (direct delivery of green fluorescence-labeled C6 dye into the inner ear through a surgical approach in the semicircular canal), and tympanic Gel + C6 (injection of in situ hydrogel loaded with green fluorescence-labeled C6 dye into the middle ear). Both the semicircular C6 and tympanic Gel + C6 treatments displayed similar and robust green fluorescence (Figure 7c and d), suggesting that intratympanic injection of an in situ hydrogel loaded with green fluorescence labeled C6 dye facilitates efficient penetration into the inner ear.

The results demonstrate the effective intratympanic delivery of BDNF-PLGA-loaded hydrogel into the inner ear, resulting in the activation of the TRKB signaling pathway. Additionally, this study provides evidence of sustained and high-dose BDNF release from the middle ear to the inner ear, as indicated by the activation of the downstream BDNF receptor, TRKB.[63,64] Additionally, the use of green fluorescence-labeled C6 dye allowed us to visualize the permeability of the drug-loaded hydrogel, demonstrating the ability of drugs encapsulated in hydrogels to reach the inner ear at high concentrations.[62,65] This confirms that drugs encapsulated in hydrogels in the middle ear can effectively reach the inner ear at high concentrations, which is a critical finding introduced in this study.

Total Excretion of Temperature-Sensitive Hydrogel-Loaded BDNF-PLGA via the Eustachian Tube. To assess the excretion capability of the thermally reversible in situ hydrogel loaded with BDNF-PLGA through the eustachian tube, we performed intratympanic injection of the hydrogel dyed with SUGARMAN food coloring (fruit green). This allowed us to visualize the discharge process of the hydrogel via the eustachian tube in response to temperature changes, and the residual green hydrogel was quantified in the tympanum. The tympanic photoimages were captured at various temperatures and time points after the intratympanic injection, as shown in Figure 8a and b(A−D). We observed that the green hydrogel could not be excreted via the eustachian tube within the temperature range from 30.5 to 37 °C due to its gel state. However, intermittent icing treatment (8−12 h, 10 min per hour, <30.5 °C) facilitated complete metabolism of the hydrogel loaded with BDNF-PLGA-SUGARMAN through the eustachian tube.

The residual mass percentage of the green hydrogel was quantified in the tympanic chamber (<30.5 °C) after intermittent icing treatment, as shown in Figure 8c(A′−D′). The remaining mass ratios at different time points were as follows: 98.33 ± 0.88 (1 h), 64.67 ± 1.76 (2 h), 55.00 ± 1.53 (3 h), 43.00 ± 1.53 (4 h), 35.00 ± 1.53 (5 h), 31.00 ± 1.53 (6 h), 18.33 ± 1.76 (7 h), 8.33 ± 1.45 (8 h), 5.67 ± 0.44 (9 h), 3.33 ± 0.33 (10 h), 3.00 ± 0.58 (11 h), and 3.00 ± 0.00 (12 h). These results demonstrate a gradual decrease in the residual hydrogel in the middle ear with intermittent icing treatment, leading to complete excretion of the hydrogel within 8−12 h.

To ensure the safety of intratympanic injection of the thermally reversible in situ hydrogel, we monitored the dynamic changes in the tympanic membrane using endoscopic images. Our observations revealed complete repair of the tympanic membranes on day 14 after injection (Figure S10a−j). This study supports the notion that our intratympanic-injected inner ear drug delivery system has no long-term detrimental effect on the tympanic membrane and the middle ear.

Certain pharmaceuticals, like glucocorticoids, have demonstrated effectiveness in treating NIHL or cochlear synaptopathy when directly administered at high doses directly to the inner ear.[65−67] Nonetheless, the systemic use of glucocorticoids (intravenous, intramuscular, or oral) can lead to severe side effects, thereby limiting their clinical value. In this study, we tackled this challenge by utilizing PLGA microspheres to load high dosages of BDNF. These microspheres were then combined with a solution at a lower temperature, resulting in the creation of injectable PLGA-PEG-PLGA hydrogels specifically designed for middle ear delivery. This innovative approach aims to enhance the therapeutic potential of BDNF while mitigating systemic side effects, rendering it a promising strategy for treating NIHL and cochlear synaptopathy. Compared to glucocorticoids, BDNF demonstrates a superior safety profile in the treatment of NIHL,[23,68] particularly in terms of restoring ribbon synaptic loss. This underscores the potential of BDNF-based therapy as a safer and more effective alternative for addressing the challenges posed by NIHL and associated cochlear synaptopathy. This study demonstrates the high therapeutic efficacy of BDNF-loaded thermosensitive hydrogels in treating sensorineural deafness, resulting in a significant recovery in the ribbon synapse and complete restoration of hearing thresholds. Additionally, this study has showed that the thermosensitive properties of PLGA-PEG-PLGA hydrogel can be successfully utilized in the middle ear to achieve prolonged BDNF release and attain a highly effective therapeutic outcome. In contrast, a previous study suggested that intratympanic injection of dexamethasone alone could partially restore hearing loss.[29] However, water-soluble dexamethasone injected into the middle ear is likely to be rapidly excreted through the eustachian tube, preventing the maintenance of high doses or sustained drug release.

To provide a comprehensive understanding, our investigation visualized the entire process of P-G hydrogels loaded with BDNF, including entry into the middle ear, residence, and eventual excretion. Both PLGA-PEG-PLGA and PLGA microspheres are biodegradable under physiological conditions through hydrolysis, cleaving the ester bonds of polymer chains.[69,70] Importantly, our study showed minimal hydrogel residues in the middle ear attributed to the sol−gel−sol transition property, allowing for excretion via the eustachian tube.

Study Limitations. The limitations of this study are as follows: (1) The thermosensitive hydrogels in this study need

https://doi.org/10.1021/acsnano.3c11049
ACS Nano XXXX, XXX, XXX−XXX

to be further optimized to achieve better adaptation to the properties of the middle ear cavity and to improve the entry efficiency of the loaded drugs into the inner ear. (2) Based on this hydrogel delivery system, we only investigated the effect of BDNF entry into the inner ear to treat NIHL and overlooked other drug candidates for testing. In the future, investigators should use this hydrogel delivery system for drug screening and verification. (3) This study used only mouse models for validation; multiple types of animals, particularly large animal models, are required in further studies. (4) This study investigated the therapeutic effect of a BDNF-loaded hydrogel delivery system under NIHL conditions, and the time course of the therapeutic effect verification may not be sufficient. Moreover, this study does not explore the effects of other deafness scenarios. Future studies should attempt to apply this drug-loaded hydrogel delivery system to other applications.

CONCLUSION

Our study demonstrates a successful, minimally invasive, single-dose, and controllable middle ear drug delivery system using a degradable thermally reversible BDNF-PLGA-loaded hydrogel, effectively repairing cochlear synaptopathy. This approach offers promising prospects for treating sensorineural deafness, representing a notable advancement in hearing treatment via targeted drug-loaded hydrogel injections. The findings lay the foundation for future research in sensorineural deafness treatment.

MATERIALS AND METHODS

Material Synthesis and Reagents. Triblock copolymers PLGA-PEG-PLGA (2.5/1, PEG Mn = 2000, PLGA Mn = 4000, Daigang Biotechnology China Co., Ltd.) were dissolved in deionized (DI) water and magnetically stirred at 4 °C until completely dissolved. Recombinant human BDNF protein (Bio-Techne China Co., Ltd., 248-BDB-250/CF) was dissolved in double distilled water (ddH_2O) as a stock (250 ug/mL) and stored at −20 °C. Before use, an appropriate amount of BDNF stock solution was diluted with ddH2O to the corresponding concentration. Coumarin 6 (MCE Chemicals & Equipment Co., Malta, NY, HY-N7131) was dissolved in DMSO as a stock solution (10 mM/mL) and stored at −80 °C. Before use, coumarin 6 was diluted to 10 uM/mL with phosphate-buffered saline (PBS). SUGARMAN Green Nature Pigment (Guangzhou Fuzheng Donghai Food China Co. Ltd., 7801536) was dissolved in DI water (1,10), stored at room temperature, and used to visualize the thermally reversible in situ hydrogel in tympanic membrane endoscopic images (Telecam DXII, Storz). The composition of the intratympanic injection appliance includes a microinjector (10 μL, Model 1701 LT SYR, Hamilton, 80001) and a backfilling blunt needle (30 gauge, 2" long, Drummond, 3−000−027).

Phase Diagram. The sol−gel transition temperature of PLGA-PEG-PLGA was tested by a vial inversion approach. Triblock copolymer aqueous solutions with concentrations ranging from 15% (w/v) to 25% (w/v) were prepared and stored at 4 °C. Subsequently, 0.5 mL of polymer solution was transferred to a 5 mL vial placed in a water bath with precise temperature control. The temperature was incrementally raised to 1 °C, and each temperature was held for 10 min. The test range spanned from 20 to 70 °C. Upon vial inversion, the PLGA-PEG-PLGA solution did not flow and could be maintained for more than 30 s, signifying the determination of the sol−gel phase transition temperature of PLGA-PEG-PLGA solution at this concentration.

Dynamic Rheological Measurement. The dynamic rheology properties of the PLGA-PEG-PLGA aqueous solutions were measured by a MCR 301 (Anton-Paar, Graz, Austria). Temperature sweeps were carried out with a heating rate of 1 °C/min, ranging from 10 to 70 °C. The strain amplitude was set at 1%, and angular frequency was set at 6 rad/s. Time sweeps were performed to monitor in situ gelation at 37 °C and mechanical properties at 1% strain amplitude and angular frequencies of 6 rad/s.

In Vitro Biodegradation. In vitro biodegradation tests of hydrogel-loaded BDNF-PLGA were conducted in PBS. Circular samples with a diameter of 1 cm and a thickness of 1 mm were precisely weighed and immersed in PBS at 37 °C. At various time intervals, the samples were removed from PBS, excess water was carefully removed from the surface using filter paper, and their weights were recorded. The remaining mass percentage was calculated by comparing the recorded weight to the original weight. Each data point was based on three parallel samples to ensure accuracy and reliability.

Preparation of Thermosensitive Hydrogel-Loaded BDNF-PLGA Systems. BDNF was loaded into poly(lactide-*co*-glycolide) (PLGA) microspheres through a specific process. BDNF was dissolved in DI water at a concentration of 50 μg/mL to serve as the internal water phase, while PLGA (52 000) was dissolved in DCM to create a PLGA solution at a concentration of 60 g/L as the oil phase. A PVA aqueous solution with a concentration of 10 g/L was used as the outer water phase. The internal water phase (50 μL) was mixed with the oil phase (1 mL) and subjected to 100W ultrasonication for 2 min in an ice bath. This mixture was then added drop by drop into a 20 mL of PVA solution. After the DCM was volatilized, the solution was centrifuged at 8000 rpm, resulting in BDNF-loaded PLGA microspheres. To observe the morphology and size of the microspheres, they were dispersed in water and deposited on a carbon-coated copper net for natural drying, followed by examination with transmission electron microscopy. The preparation method was repeated, but the dosage of bovine serum albumin (BSA) was adjusted to 6.5 mg. Furthermore, Gel-BDNF-SUGARMAN was obtained by dissolving the thermosensitive hydrogel loaded with BDNF-PLGA in DI water containing SUGARMAN. Similarly, Gel-C6 was formed by dissolving PLGA-PEG-PLGA in deionized water containing green fluorescence labeled C6 dye.

In Vitro Release Profile. BSA dissolved in PBS buffer at different concentrations was tested by a microplate reader (PerkinElmer, Waltham, MA, USA). The standard curve of BSA (Abs = 0.0022 × concentration + 0.066) was obtained by fitting the absorbance at 562 nm as a function of concentration by the Micro BCA method. The drug release profile was measured with a customized diffusion cell system. We placed PLGA-PEG-PLGA hydrogel containing PLGA-BDNF microspheres on the top of a semipermeable membrane and the receptor fluid (PBS buffer) on the bottom at 37 °C. The receiving solution was sampled and supplemented periodically. Based on the standard curve, accumulative drug release profiles were achieved.

Animals and Grouping. The experiments were performed on four-week-old male C57BL/6J mice to exclude the influence of gender on the results. A total of 96 mice with normal hearing were purchased from SPF Biotechnology Co., Ltd. (Beijing, China; Experimental Animal License no. SCXK (Beijing) 2019−0010). Before the experiments, the animals were tested to ensure the absence of external or middle ear pathology and were group-housed in a standard 12:12 h light−dark cycle with a constant climate and had free access to water and food.

According to different intervention strategies, the mice were randomly divided into the following groups:

1. A control group not given any treatment (Ctrl, n = 3) and a hydrogel group given an intratympanic injection of PLGA-PEG-PLGA hydrogel alone (Gel, 10 ul/ear, n = 3). Hearing detection was performed in both groups on days 1, 7, and 14 after tympanic chamber injection.
2. A control group (Ctrl, n = 15), a 4 h noise exposure group (NE, white noise, 115 dB SPL, n = 21), a semicircular canal administration of the BDNF within 14 h after NE group (NE + BDNF′, 25 ug/mL, 2 ul/ear, n = 6), an intratympanic injection of the BDNF group within 14 h after NE (NE + BDNF, 25 ug/mL, 10 ul/ear, n = 9), and an intratympanic injection of the temperature-sensitive type in situ hydrogel-loaded BDNF-PLGA group within 14 h after NE (NE + Gel-BDNF, 50 ug/

https://doi.org/10.1021/acsnano.3c11049
ACS Nano XXXX, XXX, XXX−XXX

mL, 10 ul/ear, n = 12). All groups were detected for ABR hearing thresholds on days 2, 7, and 14 after NE, and immunofluorescence staining was performed on day 14. Western blot was performed on day 2 after NE in the NE and NE + BDNF groups.

3. A semicircular canal to introduce the green fluorescence-labeled C6 dye group (Semicircular C6, 2 ul/ear, n = 3), an intratympanic injection hydrogel loaded with green fluorescence-labeled C6 dye group (Tympanic Gel+C6, 10 ul/ear, n = 3), and an intratympanic injection green fluorescence-labeled C6 dye group (Tympanic C6, 10 ul/ear, n = 3). Immunofluorescence staining was performed in all groups 1 day after drug administration.
4. A 4 h noise exposure group (NE, n = 3) and an intratympanic injection of the thermally reversible in situ hydrogel loaded with BDNF-PLGA dyed with SUGARMAN food coloring (fruit green) group after NE (NE + Gel-BDNF-SUGARMAN, 10 ul/ear, n = 18). The green hydrogel remaining mass percentage in the tympanum at different periods was quantified on the 14th day after NE.
5. The animals were cared for and used following the Guideline for the Care and Use of Laboratory Animals of the National Institutes of Health. The experimental protocols were approved by the Committee on the Ethics of Animal Experiments of Capital Medical University (AEEI-2021−298).

Noise Exposure. Animals in the noise group were placed in wire mesh cages inside an anechoic chamber and exposed to 115 dB sound pressure level (SPL) broadband white noise for 4 h. Noise synthesis was performed using Cool Edit Pro software (Adobe Systems, San Jose, CA) and transmitted through XTi4002 CROWN amplifiers (Harman, Elkhart, IN) to two speakers (JBL KP6000, PROFESSIONAL, Harman) for noise release.

Auditory Brainstem Responses. All animals were anesthetized via intraperitoneal injection of ketamine (100 mg/kg, Gutian Pharmaceutical Co., Ltd., Fujian, China) and xylazine (10 mg/kg, Sigma-Aldrich Co., Llc., United States). Needle electrodes were placed subcutaneously beneath the pinna of the test ear (−) and at the vertex (+), with a ground electrode placed in the contralateral ear over the neck muscles. The ABR threshold was recorded in a double-walled, electrically shielded, and radio frequency-shielded sound booth. ABR stimulus frequencies of 4, 8, 16, and 32 kHz and clicks (100 μs) were tested with system 3 hardware (Tucker Davis Technologies, Alachua, FL, United States) and SigGen/BioSig software (Tucker Davis Technologies). The stimulus level was calibrated, and a probe tube microphone was tightly fitted into the external auditory canal.

The ABR threshold was obtained for each animal by reducing the stimulus intensity in 10 dB steps and then 5 dB steps to identify the lowest intensity eliciting a response. The ABR threshold was defined as the lowest stimulus intensity that produced reliable and reproducible (in at least two trials) ABR waves. The amplitude of wave I was identified as the difference between the first peak in the waveform and the baseline.

In Vitro Culture of the Cochlea Basilar Membrane. P5 C57BL/6J mice were euthanized using carbon dioxide and disinfected with 75% ethanol. Their heads were then removed, and the brain tissue was separated. Under a stereoscopic anatomical microscope, the cochlear structure was isolated and the basilar membrane of the cochlea was rapidly dissected. Subsequently, the basilar membrane was transferred into Dulbecco's modified Eagle medium (DMEM)/F12 (containing penicillin) medium (Sigma-Aldrich, St. Louis, USA) supplemented with 10% bovine serum albumin (Sigma-Aldrich) and incubated for 24 h at 37 °C in 95% oxygen and 5% CO_2. After 1 day of in vitro cultivation, the cochlear explants were used in the subsequent experiments.

The cochlear explants of the control group (Ctrl) remained in the DMEM/F12 medium for 3 and 5 days, with the medium being replaced daily. The cochlear explants of the PLGA-PEG-PLGA hydrogel group (Gel) were kept in the DMEM/F12 medium for 24 h and then transferred to the DMEM/F12 medium containing PLGA-PEG-PLGA hydrogel (20 mg/mL) for 3 and 5 days, with the medium being replaced daily.[71] To examine excitotoxic damage, which is a type of noise-induced synaptic disorder, the explants were incubated in the DMEM/F12 (containing penicillin) medium for 24 h and then treated with 0.5 mM NK medium for 12 h. The NK medium consisted of 0.5 mM *N*-methyl-D-aspartate (0114, Tocris Bioscience, UK) and 0.5 mM kainate (K2389, Sigma-Aldrich, USA). To simulate the in vitro therapeutic effect of BDNF after noise exposure (NK + BDNF), the explants were first cultured in the 0.5 mM NK medium for 12 h and then in the 10 nM BDNF medium for 24 h. After the experiments, the cochleae of all four groups were removed from the medium and immobilized for further analysis.

Immunofluorescence Staining. Animals were decapitated under anesthesia (ketamine, 100 mg/kg, ip; and xylazine, 10 mg/kg i.p.). Cochlear tissues were carefully removed and initially fixed with 4% paraformaldehyde in phosphate-buffered saline (PBS) overnight at 4 °C. After fixation, the cochlea were decalcified with 10% EDTA for 1−2 h. Then the apical, middle, and basal turns of the basilar membrane were separated in PBS with vestibular membrane and the tectorial membrane removed. Specimens were subsequently incubated with 0.3% Triton X-100 in 0.2 M PBS for 30 min and 10% goat serum (ZSGB-BIO) for 1 h at room temperature. Specimens were incubated overnight at 4 °C with the following primary antibodies: rabbit antimyosin-VIIa antibody (1:300, Proteus BioSciences Inc., 25−6790), mouse anti-CtBP2 antibody (1:500, Abcam, ab204663), mouse anti-GluR2 antibody (1:400, Millipore, MAB397), and chicken anti-NF200 (neurofilament 200) antibody (1:400, Chemicon, AB5539). The next day, the specimens were rinsed three times in PBS for 10 min each and then incubated with secondary antibodies conjugated with goat antirabbit IgG (H + L) Alexa Fluor 647/488, goat antimouse IgG1 Alexa Fluor 568, and goat antimouse IgG2a Alexa Fluor 488 (1:300, Invitrogen, A-21245, A-21124, and A-21131, respectively), along with goat anti-Chicken IgY (H + L) Alexa Fluor 594 (1:300, Abcam, ab150176), for an additional 2 h at room temperature, then washed three times with PBS for 10 min each and mounted on a glass coverslip with DAPI (ZSGB-BIO, ZLI-9557).

Confocal Microscope Imaging. Images were captured using a 63× oil-immersion, high-resolution confocal microscope (TCS SP8 II; Leica Microsystems, Wetzlar, Germany). Scanning was conducted from top to bottom with an interval of 0.5 μm per layer, resulting in a series of z-stack images. The specimens were observed with optimal excitation wavelengths of 488 (green), 568 (red), and 647 nm (silver gray). DAPI staining was visualized using an optimal excitation wavelength of 358 nm (blue).

Calculation of the Number and Size of Ribbon Synapses. Quantification of auditory nerve fibers (ANFs), labeled by anti-NF200, and ribbon synapses, labeled by anti-GluR2 and anti-CtBP2, was conducted on the 14th day after NE. Additionally, the number of ribbon synapses was quantified in the cochlear apex turn, middle turn, and basal turn. Four samples were selected in each group to calculate the average number of ribbon synapses for each inner hair cell (IHC). The total numbers of GluR2- and CtBP2-stained puncta were combined and divided by the total number of IHC nuclei. The merged areas of pre- and postsynaptic ribbons were measured using Adobe Photoshop CS6 software. The synaptic elements were segmented from the whole image into a single area, and the area of the synapse was obtained by using the measurement area tool.

Counting the Number of Hair Cells. Quantification of outer hair cells (OHCs) and inner hair cells (IHCs) was performed in the cochlear apex turn, middle turn, and basal turn. A hair cell was considered present if it had an intact, spherical nucleus located in the basal half of the cell. When the tissue was photographed, special care was taken to ensure that the nuclei in the focal segment belonged to the OHCs and not nearby supporting cells. In DAPI-labeled tissue, intact spherical nuclei were counted to estimate the number of OHCs and IHCs. For each basilar turn, three visual fields were selected, each containing approximately 10−14 IHCs and 30−42 OHCs. Four samples were chosen in each group to calculate the average number of OHCs and IHCs. OHCs and IHCs counts from confocal images were

https://doi.org/10.1021/acsnano.3c11049
ACS Nano XXXX, XXX, XXX−XXX

conducted using ImageJ software (ver. 1.37, NIH, Wayne Rasband, USA).

Western Blot Analysis. Hank's balanced salt solution (Gibco, 1491037) was used to dissect the cochlea immediately after removal. The cochlea was homogenized in ice-cold RIPA lysis solution (G2002, Servicebio) containing phosphatase inhibitor cocktails and a RIPA lysis buffer base (G2007, Servicebio). After 30 min on ice, tissue fragments were separated by centrifugation at 12 000 g for 10 min at 4 °C, and the supernatants were collected as the total protein fractions. Protein concentrations were measured using the BCA Protein Assay Kit (G2026, Servicebio). For each sample, two cochlea from the same mouse were combined. Primary antibody concentrations used were anti-TRKB (1:2000; Immunoway, YP0270) and anti-ACTIN (1:12000; Immunoway, YM0012). Protein samples (10 μL) were separated using SDS-PAGE (G2003, Servicebio) and then transferred onto nitrocellulose after electrophoresis. The membrane was blocked using a 5% nonfat dry milk solution in 0.5% TBST. Primary antibodies against TRKB (1:2000) or anti-ACTIN (1:12000) were applied to the membranes for overnight incubation at 4 °C, followed by three TBST washes lasting 10 min each. Secondary antibodies were applied to the membranes and incubated for 1 h at a concentration of 1:14000. The membrane was thoroughly washed before the immunoreactive bands were visualized using ECL. X-ray films of Western blots were scanned and examined using AlphaEase FC software. The relative expression levels of several samples were determined by calculating the optical density ratio of the TRKB band within the ACTIN bands.

Statistical Analysis. Statistical analysis was conducted using GraphPad Prism 8 software (GraphPad Software Inc., La Jolla, CA, United States). Normally distributed continuous variables were presented as means ± standard error of the mean (SEM). Statistical differences between groups were analyzed using two-way analysis of variance (ANOVA), followed by Bonferroni's multiple comparisons test. For all analyses, values of $p < 0.05$ were considered statistically significant. *$p < 0.05$, **$p < 0.01$, ***$p < 0.001$, and ****$p < 0.0001$.

ASSOCIATED CONTENT

Data Availability Statement

All data needed to evaluate the conclusions in the paper are present in the paper and/or the Supporting Information. Additional data related to this paper are available from the corresponding authors upon request.

Supporting Information

The Supporting Information is available free of charge at https://pubs.acs.org/doi/10.1021/acsnano.3c11049.

Schematics of the experimental procedure, immunostaining results, hair cell counts, hearing detection results, quantitative analysis of ribbon synaptic spots, ABR data, and wave I waveforms (PDF)

AUTHOR INFORMATION

Corresponding Authors

Ke Liu − *Department of Otolaryngology Head and Neck Surgery, Beijing Friendship Hospital and Clinical Center for Hearing Loss, Capital Medical University, Beijing 100050, China;* orcid.org/0000-0002-0505-920X; Email: liuke@ccmu.edu.cn

Lan Yin − *School of Materials Science and Engineering, Tsinghua University, Beijing 100084, China;* orcid.org/0000-0001-7306-4628; Email: lanyin@tsinghua.edu.cn

Authors

Qianru Yu − *Department of Otolaryngology Head and Neck Surgery, Beijing Friendship Hospital, Capital Medical University, Beijing 100050, China*

Shengnan Liu − *School of Materials Science and Engineering, Tsinghua University, Beijing 100084, China*

Rui Guo − *Department of Otolaryngology Head and Neck Surgery, Beijing Friendship Hospital, Capital Medical University, Beijing 100050, China;* orcid.org/0000-0002-6708-526X

Kuntao Chen − *School of Materials Science and Engineering, Tsinghua University, Beijing 100084, China*

Yang Li − *Department of Otolaryngology Head and Neck Surgery, Beijing Friendship Hospital, Capital Medical University, Beijing 100050, China*

Dan Jiang − *Hearing Implant Centre, Guy's and St. Thomas NHS Foundation Trust, London SE1 7EH, United Kingdom; Centre for Craniofacial and Regenerative Biology, King's College London, London SE1 9RT, United Kingdom*

Shusheng Gong − *Department of Otolaryngology Head and Neck Surgery, Beijing Friendship Hospital and Clinical Center for Hearing Loss, Capital Medical University, Beijing 100050, China*

Complete contact information is available at: https://pubs.acs.org/10.1021/acsnano.3c11049

Author Contributions

▽These authors contributed equally to this work. Q.Y., S.L., R.G., K.C., Y.L., D.J., S.G., K.L., and L.Y conceptualized the project.; Q.Y. R.G.,Y.L., D.J., S.G., and K.L designed and conducted animal testing; S.L., K.C., and L.Y designed and fabricated the hydrogels and tested drug sustained-release system; Q.Y. R.G., Y.L., S.L., and K.C collected the data. Q.Y., S.L., K.L., and L.Y performed data analysis; Q.Y. R.G., Y.L., S.L., and K.C developed photographs and schematic diagrams in the manuscript; and Q.Y. and K.L wrote the manuscript with inputs from all authors. All the authors discussed the results and commented on the manuscript. All authors reviewed and approved the final version of the manuscript.

Funding

National Natural Science Foundation of China (82071037, 81830030).

Notes

The authors declare no competing financial interest.

ACKNOWLEDGMENTS

We thank all members of the Auditory laboratory for many helpful discussions and support throughout this project; particularly, thanks to Professor Liu Ke for his careful guidance and Wang Jingjing for providing the public laboratory platform for immunofluorescence experiments.

REFERENCES

(1) Chadha, S.; Kamenov, K.; Cieza, A. The world report on hearing, 2021. *Bull. World Health Organ.* **2021**, *99* (4), 242−242A.

(2) Kujawa, S. G.; Liberman, M. C. Adding insult to injury: cochlear nerve degeneration after "temporary" noise-induced hearing loss. *J. Neurosci.* **2009**, *29* (45), 14077−14085.

(3) Petitpré, C.; Wu, H.; Sharma, A.; Tokarska, A.; Fontanet, P.; Wang, Y.; Helmbacher, F.; Yackle, K.; Silberberg, G.; Hadjab, S.; Lallemend, F. Neuronal heterogeneity and stereotyped connectivity in the auditory afferent system. *Nat. Commun.* **2018**, *9*, 3691.

(4) Verbeek, J. H.; Kateman, E.; Morata, T. C.; Dreschler, W.; Sorgdrager, B. Interventions to prevent occupational noise-induced hearing loss. *Cochrane Database Syst. Rev.* **2009**, No. 3, CD006396.

(5) Lobarinas, E.; Spankovich, C.; Le Prell, C. G. Evidence of "hidden hearing loss" following noise exposures that produce robust

TTS and ABR wave-I amplitude reductions. *Hear Res.* **2017**, *349*, 155−163.
(6) Bakay, W. M. H.; Anderson, L. A.; Garcia-Lazaro, J. A.; McAlpine, D.; Schaette, R. Hidden hearing loss selectively impairs neural adaptation to loud sound environments. *Nat. Commun.* **2018**, *9*, 4298.
(7) Shi, L.; Chang, Y.; Li, X.; Aiken, S.; Liu, L.; Wang, J. Cochlear Synaptopathy and Noise-Induced Hidden Hearing Loss. *Neural Plast.* **2016**, *2016*, 6143164.
(8) Kobel, M.; Le Prell, C. G.; Liu, J.; Hawks, J. W.; Bao, J. Noise-induced cochlear synaptopathy: Past findings and future studies. *Hear Res.* **2017**, *349*, 148−154.
(9) Liberman, M. C.; Kujawa, S. G. Cochlear synaptopathy in acquired sensorineural hearing loss: Manifestations and mechanisms. *Hear Res.* **2017**, *349*, 138−147.
(10) Liu, K.; Jiang, X.; Shi, C.; Shi, L.; Yang, B.; Shi, L.; Xu, Y.; Yang, W.; Yang, S. Cochlear inner hair cell ribbon synapse is the primary target of ototoxic aminoglycoside stimuli. *Mol. Neurobiol.* **2013**, *48* (3), 647−654.
(11) Luo, Y.; Qu, T.; Song, Q.; Qi, Y.; Yu, S.; Gong, S.; Liu, K.; Jiang, X. Repeated Moderate Sound Exposure Causes Accumulated Trauma to Cochlear Ribbon Synapses in Mice. *Neuroscience.* **2020**, *429*, 173−184.
(12) Wei, W.; Shi, X.; Xiong, W.; He, L.; Du, Z. D.; Qu, T.; Qi, Y.; Gong, S. S.; Liu, K.; Ma, X. RNA-seq Profiling and Co-expression Network Analysis of Long Noncoding RNAs and mRNAs Reveal Novel Pathogenesis of Noise-induced Hidden Hearing Loss. *Neuroscience.* **2020**, *434*, 120−135.
(13) Sha, S. H.; Schacht, J. Emerging therapeutic interventions against noise-induced hearing loss. *Expert Opin Investig Drugs* **2017**, *26* (1), 85−96.
(14) Salt, A. N.; Plontke, S. K. Local inner-ear drug delivery and pharmacokinetics. *Drug Discov Today.* **2005**, *10* (19), 1299−1306.
(15) Landegger, L. D.; Pan, B.; Askew, C.; Wassmer, S. J.; Gluck, S. D.; Galvin, A.; Taylor, R.; Forge, A.; Stankovic, K. M.; Holt, J. R.; Vandenberghe, L. H. A synthetic AAV vector enables safe and efficient gene transfer to the mammalian inner ear. *Nat. Biotechnol.* **2017**, *35* (3), 280−284.
(16) Yeo, B. S. Y.; Song, H. J. J. M. D.; Toh, E. M. S.; Ng, L. S.; Ho, C. S. H.; Ho, R.; Merchant, R. A.; Tan, B. K. J.; Loh, W. S. Association of Hearing Aids and Cochlear Implants With Cognitive Decline and Dementia: A Systematic Review and Meta-analysis. *JAMA Neurol.* **2023**, *80* (2), 134−141.
(17) Mathiesen, B. K.; Miyakoshi, L. M.; Cederroth, C. R.; Tserga, E.; Versteegh, C.; Bork, P. A. R.; Hauglund, N. L.; Gomolka, R. S.; Mori, Y.; Edvall, N. K.; Rouse, S.; Møllgård, K.; Holt, J. R.; Nedergaard, M.; Canlon, B. Delivery of gene therapy through a cerebrospinal fluid conduit to rescue hearing in adult mice. *Sci. Transl Med.* **2023**, *15* (702), eabq3916.
(18) Shi, X.; Wang, Z.; Ren, W.; Chen, L.; Xu, C.; Li, M.; Fan, S.; Xu, Y.; Chen, M.; Zheng, F.; Zhang, W.; Zhou, X.; Zhang, Y.; Qiu, S.; Wu, L.; Zhou, P.; Lv, X.; Cui, T.; Qiao, Y.; Zhao, H.; et al. LDL receptor-related protein 1 (LRP1), a novel target for opening the blood-labyrinth barrier (BLB). *Signal Transduct Target Ther.* **2022**, *7*, 175.
(19) Carlson, M. L. Cochlear Implantation in Adults. *N Engl J. Med.* **2020**, *382* (16), 1531−1542.
(20) Jaumann, M.; Dettling, J.; Gubelt, M.; Zimmermann, U.; Gerling, A.; Paquet-Durand, F.; Feil, S.; Wolpert, S.; Franz, C.; Varakina, K.; Xiong, H.; Brandt, N.; Kuhn, S.; Geisler, H. S.; Rohbock, K.; Ruth, P.; Schlossmann, J.; Hütter, J.; Sandner, P.; Feil, R.; et al. cGMP-Prkg1 signaling and Pde5 inhibition shelter cochlear hair cells and hearing function. *Nat. Med.* **2012**, *18* (2), 252−259.
(21) Cunningham, L. L.; Tucci, D. L. Restoring synaptic connections in the inner ear after noise damage. *N Engl J. Med.* **2015**, *372* (2), 181−182.
(22) Park, H.; Poo, M. M. Neurotrophin regulation of neural circuit development and function. *Nat. Rev. Neurosci.* **2013**, *14* (1), 7−23.
(23) Cao, T.; Matyas, J. J.; Renn, C. L.; Faden, A. I.; Dorsey, S. G.; Wu, J. Function and Mechanisms of Truncated BDNF Receptor TrkB.T1 in Neuropathic Pain. *Cells.* **2020**, *9* (5), 1194.
(24) Lima Giacobbo, B.; Doorduin, J.; Klein, H. C.; Dierckx, R. A. J. O.; Bromberg, E.; de Vries, E. F. J. Brain-Derived Neurotrophic Factor in Brain Disorders: Focus on Neuroinflammation. *Mol. Neurobiol.* **2019**, *56* (5), 3295−3312.
(25) Holt, L. M.; Hernandez, R. D.; Pacheco, N. L.; Torres Ceja, B.; Hossain, M.; Olsen, M. L. Astrocyte morphogenesis is dependent on BDNF signaling via astrocytic TrkB.T1. *eLife* **2019**, *8*, e44667.
(26) Lilius, T. O.; Blomqvist, K.; Hauglund, N. L.; Liu, G.; Stæger, F. F.; Bærentzen, S.; Du, T.; Ahlström, F.; Backman, J. T.; Kalso, E. A.; Rauhala, P. V.; Nedergaard, M. Dexmedetomidine enhances glymphatic brain delivery of intrathecally administered drugs. *J. Controlled Release* **2019**, *304*, 29−38.
(27) Nyberg, S.; Abbott, N. J.; Shi, X.; Steyger, P. S.; Dabdoub, A. Delivery of therapeutics to the inner ear: The challenge of the blood-labyrinth barrier. *Sci. Transl Med.* **2019**, *11* (482), eaao0935.
(28) Zhang, W.; Dai, M.; Fridberger, A.; Hassan, A.; Degagne, J.; Neng, L.; Zhang, F.; He, W.; Ren, T.; Trune, D.; Auer, M.; Shi, X. Perivascular-resident macrophage-like melanocytes in the inner ear are essential for the integrity of the intrastrial fluid-blood barrier. *Proc. Natl. Acad. Sci. U. S. A.* **2012**, *109* (26), 10388−10393.
(29) Wang, J.; Wang, C.; Wang, Q.; Zhang, Z.; Wang, H.; Wang, S.; Chi, Z.; Shang, L.; Wang, W.; Shu, Y. Microfluidic Preparation of Gelatin Methacryloyl Microgels as Local Drug Delivery Vehicles for Hearing Loss Therapy. *ACS Appl. Mater. Interfaces.* **2022**, *14* (41), 46212−46223.
(30) Gausterer, J. C.; Saidov, N.; Ahmadi, N.; Zhu, C.; Wirth, M.; Reznicek, G.; Arnoldner, C.; Gabor, F.; Honeder, C. Intratympanic application of poloxamer 407 hydrogels results in sustained N-acetylcysteine delivery to the inner ear. *Eur. J. Pharm. Biopharm.* **2020**, *150*, 143−155.
(31) Paulson, D. P.; Abuzeid, W.; Jiang, H.; Oe, T.; O'Malley, B. W.; Li, D. A novel controlled local drug delivery system for inner ear disease. *Laryngoscope.* **2008**, *118* (4), 706−711.
(32) El Kechai, N.; Agnely, F.; Mamelle, E.; Nguyen, Y.; Ferrary, E.; Bochot, A. Recent advances in local drug delivery to the inner ear. *Int. J. Pharm.* **2015**, *494* (1), 83−101.
(33) Girish, K. S.; Kemparaju, K. The magic glue hyaluronan and its eraser hyaluronidase: a biological overview. *Life Sci.* **2007**, *80* (21), 1921−1943.
(34) Kim, Y. M.; Park, M. R.; Song, S. C. Injectable polyplex hydrogel for localized and long-term delivery of siRNA. *ACS Nano* **2012**, *6* (7), 5757−5766.
(35) Rahmani, F.; Atabaki, R.; Behrouzi, S.; Mohamadpour, F.; Kamali, H. The recent advancement in the PLGA-based thermo-sensitive hydrogel for smart drug delivery. *Int. J. Pharm.* **2023**, *631*, 122484.
(36) Wang, P.; Chu, W.; Zhuo, X.; Zhang, Y.; Gou, J.; Ren, T.; He, H.; Yin, T.; Tang, X. Modified PLGA-PEG-PLGA thermosensitive hydrogels with suitable thermosensitivity and properties for use in a drug delivery system. *J. Mater. Chem. B* **2017**, *5* (8), 1551−1565.
(37) Ramazani, F.; Chen, W.; van Nostrum, C. F.; Storm, G.; Kiessling, F.; Lammers, T.; Hennink, W. E.; Kok, R. J. Strategies for encapsulation of small hydrophilic and amphiphilic drugs in PLGA microspheres: State-of-the-art and challenges. *Int. J. Pharm.* **2016**, *499* (1−2), 358−367.
(38) Bae, S. E.; Son, J. S.; Park, K.; Han, D. K. Fabrication of covered porous PLGA microspheres using hydrogen peroxide for controlled drug delivery and regenerative medicine. *J. Controlled Release* **2009**, *133* (1), 37−43.
(39) Zhao, D.; Li, D.; Quan, F.; Zhou, Y.; Zhang, Z.; Chen, X.; He, C. Rapidly Thermoreversible and Biodegradable Polypeptide Hydrogels with Sol-Gel-Sol Transition Dependent on Subtle Manipulation of Side Groups. *Biomacromolecules.* **2021**, *22* (8), 3522−3533.
(40) Pochan, D. J.; Schneider, J. P.; Kretsinger, J.; Ozbas, B.; Rajagopal, K.; Haines, L. Thermally reversible hydrogels via

https://doi.org/10.1021/acsnano.3c11049
ACS Nano XXXX, XXX, XXX−XXX

intramolecular folding and consequent self-assembly of a de novo designed peptide. *J. Am. Chem. Soc.* **2003**, *125* (39), 11802−11803.
(41) Jeong, B.; Bae, Y. H.; Lee, D. S.; Kim, S. W. Biodegradable block copolymers as injectable drug-delivery systems. *Nature.* **1997**, *388* (6645), 860−862.
(42) Aubert-Pouëssel, A.; Venier-Julienne, M. C.; Clavreul, A.; Sergent, M.; Jollivet, C.; Montero-Menei, C. N.; Garcion, E.; Bibby, D. C.; Menei, P.; Benoit, J. P. In vitro study of GDNF release from biodegradable PLGA microspheres. *J. Controlled Release* **2004**, *95* (3), 463−475.
(43) Lee, D. S.; Shim, M. S.; Kim, S. W.; Lee, H.; Park, I.; Chang, T. Y. Novel thermoreversible gelation of biodegradable PLGA - block - PEO - block - PLGA triblock copolymers in aqueous solution. *Macromol. Rapid Commun.* **2001**, *22*, 587−592.
(44) Nakagawa, T.; Kumakawa, K.; Usami, S.; Hato, N.; Tabuchi, K.; Takahashi, M.; Fujiwara, K.; Sasaki, A.; Komune, S.; Sakamoto, T.; Hiraumi, H.; Yamamoto, N.; Tanaka, S.; Tada, H.; Yamamoto, M.; Yonezawa, A.; Ito-Ihara, T.; Ikeda, T.; Shimizu, A.; Tabata, Y.; et al. A randomized controlled clinical trial of topical insulin-like growth factor-1 therapy for sudden deafness refractory to systemic corticosteroid treatment. *BMC Med.* **2014**, *12*, 219.
(45) Zhang, Z.; Li, X.; Zhang, W.; Kohane, D. S. Drug Delivery across Barriers to the Middle and Inner Ear. *Adv. Funct Mater.* **2021**, *31* (44), 2008701.
(46) Li, X.; Wang, Y.; Xu, F.; Zhang, F.; Xu, Y.; Tang, L.; Webster, T. J. Artemisinin Loaded mPEG-PCL Nanoparticle Based Photosensitive Gelatin Methacrylate Hydrogels for the Treatment of Gentamicin Induced Hearing Loss. *Int. J. Nanomedicine.* **2020**, *15*, 4591−4606.
(47) Feng, L.; Ward, J. A.; Li, S. K.; Tolia, G.; Hao, J.; Choo, D. I. Assessment of PLGA-PEG-PLGA copolymer hydrogel for sustained drug delivery in the ear. *Current drug delivery.* **2014**, *11* (2), 279−286.
(48) Liu, H.; Feng, L.; Tolia, G.; Liddell, M. R.; Hao, J.; Li, S. K. Evaluation of intratympanic formulations for inner ear delivery: methodology and sustained release formulation testing. *Drug Dev. Ind. Pharm.* **2014**, *40* (7), 896−903.
(49) Wang, Q.; Green, S. H. Functional role of neurotrophin-3 in synapse regeneration by spiral ganglion neurons on inner hair cells after excitotoxic trauma in vitro. *J. Neurosci.* **2011**, *31* (21), 7938−7949.
(50) Yamahara, K.; Asaka, N.; Kita, T.; Kishimoto, I.; Matsunaga, M.; Yamamoto, N.; Omori, K.; Nakagawa, T. Insulin-like growth factor 1 promotes cochlear synapse regeneration after excitotoxic trauma in vitro. *Hear Res.* **2019**, *374*, 5−12.
(51) Rutherford, M. A.; Bhattacharyya, A.; Xiao, M.; Cai, H. M.; Pal, I.; Rubio, M. E. GluA3 subunits are required for appropriate assembly of AMPAR GluA2 and GluA4 subunits on cochlear afferent synapses and for presynaptic ribbon modiolar-pillar morphology. *eLife* **2023**, *12*, e80950.
(52) Tan, W. J. T.; Song, L.; Graham, M.; Schettino, A.; Navaratnam, D.; Yarbrough, W. G.; Santos-Sacchi, J.; Ivanova, A. V. Novel Role of the Mitochondrial Protein Fus1 in Protection from Premature Hearing Loss via Regulation of Oxidative Stress and Nutrient and Energy Sensing Pathways in the Inner Ear. *Antioxid Redox Signal.* **2017**, *27* (8), 489−509.
(53) Liu, K.; Li, S.; Jiang, X. Quantitative analysis of the ribbon synapse number of cochlear inner hair cells in C57BL/6J mice using the three-dimensional modeling method. *Sci. China C Life Sci.* **2009**, *52* (9), 807−812.
(54) Wong, A. B.; Rutherford, M. A.; Gabrielaitis, M.; Pangrsic, T.; Göttfert, F.; Frank, T.; Michanski, S.; Hell, S.; Wolf, F.; Wichmann, C.; Moser, T. Developmental refinement of hair cell synapses tightens the coupling of Ca2+ influx to exocytosis. *Embo J.* **2014**, *33*, 247−264.
(55) Fernandez, K. A.; Guo, D.; Micucci, S.; De Gruttola, V.; Liberman, M. C.; Kujawa, S. G. Noise-induced Cochlear Synaptopathy with and Without Sensory Cell Loss. *Neuroscience.* **2020**, *427*, 43−57.
(56) Liberman, M. C.; Kujawa, S. G. Cochlear synaptopathy in acquired sensorineural hearing loss: Manifestations and mechanisms. *Hear Res.* **2017**, *349*, 138−147.
(57) Kujawa, S. G.; Liberman, M. C. Synaptopathy in the noise-exposed and aging cochlea: Primary neural degeneration in acquired sensorineural hearing loss. *Hear Res.* **2015**, *330*, 191−199.
(58) Liu, K.; Chen, D.; Guo, W.; Yu, N.; Wang, X.; Ji, F.; Hou, Z.; Yang, W. Y.; Yang, S. Spontaneous and Partial Repair of Ribbon Synapse in Cochlear Inner Hair Cells After Ototoxic Withdrawal. *Mol. Neurobiol.* **2015**, *52* (3), 1680−1689.
(59) Roux, I.; Safieddine, S.; Nouvian, R.; Grati, M.; Simmler, M. C.; Bahloul, A.; Perfettini, I.; Le Gall, M.; Rostaing, P.; Hamard, G.; Triller, A.; Avan, P.; Moser, T.; Petit, C. Otoferlin, defective in a human deafness form, is essential for exocytosis at the auditory ribbon synapse. *Cell.* **2006**, *127* (2), 277−289.
(60) Akil, O.; Dyka, F.; Calvet, C.; Emptoz, A.; Lahlou, G.; Nouaille, S.; Boutet de Monvel, J.; Hardelin, J. P.; Hauswirth, W. W.; Avan, P.; Petit, C.; Safieddine, S.; Lustig, L. R. Dual AAV-mediated gene therapy restores hearing in a DFNB9 mouse model. *Proc. Natl. Acad. Sci. U. S. A.* **2019**, *116* (10), 4496−4501.
(61) Xue, Y.; Li, X.; Dong, J. Interfacial characteristics of block copolymer micelles stabilized Pickering emulsion by confocal laser scanning microscopy. *J. Colloid Interface Sci.* **2020**, *563*, 33−41.
(62) Xu, B.; Zeng, F.; Deng, J.; Yao, L.; Liu, S.; Hou, H.; Huang, Y.; Zhu, H.; Wu, S.; Li, Q.; Zhan, W.; Qiu, H.; Wang, H.; Li, Y.; Yang, X.; Cao, Z.; Zhang, Y.; Zhou, H. A homologous and molecular dual-targeted biomimetic nanocarrier for EGFR-related non-small cell lung cancer therapy. *Bioact Mater.* **2023**, *27*, 337−347.
(63) Fernández-García, S.; Sancho-Balsells, A.; Longueville, S.; Hervé, D.; Gruart, A.; Delgado-García, J. M.; Alberch, J.; Giralt, A. Astrocytic BDNF and TrkB regulate severity and neuronal activity in mouse models of temporal lobe epilepsy. *Cell Death Dis.* **2020**, *11*, 411.
(64) Lin, P. Y.; Kavalali, E. T.; Monteggia, L. M. Genetic Dissection of Presynaptic and Postsynaptic BDNF-TrkB Signaling in Synaptic Efficacy of CA3-CA1 Synapses. *Cell Rep.* **2018**, *24* (6), 1550−1561.
(65) Yang, K. J.; Son, J.; Jung, S. Y.; Yi, G.; Yoo, J.; Kim, D. K.; Koo, H. Optimized phospholipid-based nanoparticles for inner ear drug delivery and therapy. *Biomaterials.* **2018**, *171*, 133−143.
(66) Tabuchi, K.; Nakamagoe, M.; Nishimura, B.; Hayashi, K.; Nakayama, M.; Hara, A. Protective effects of corticosteroids and neurosteroids on cochlear injury. *Med. Chem.* **2011**, *7* (2), 140−144.
(67) Varela-Nieto, I.; Murillo-Cuesta, S.; Calvino, M.; Cediel, R.; Lassaletta, L. Drug development for noise-induced hearing loss. *Expert Opin Drug Discovery* **2020**, *15* (12), 1457−1471.
(68) Khalin, I.; Kocherga, G.; Abu Bakar, M.; Alyautdin, R. Targeted delivery of brain-derived neurotrophic factor for the treatment of blindness and deafness. *Int. J. Nanomedicine.* **2015**, *10*, 3245−3267.
(69) Liu, Y.; Chen, X.; Li, S.; Guo, Q.; Xie, J.; Yu, L.; Xu, X.; Ding, C.; Li, J.; Ding, J. Calcitonin-Loaded Thermosensitive Hydrogel for Long-Term Antiosteopenia Therapy. *ACS Appl. Mater. Interfaces.* **2017**, *9* (28), 23428−23440.
(70) Ford Versypt, A. N.; Pack, D. W.; Braatz, R. D. Mathematical modeling of drug delivery from autocatalytically degradable PLGA microspheres–a review. *J. Controlled Release* **2013**, *165* (1), 29−37.
(71) Moser, T.; Starr, A. Auditory neuropathy–neural and synaptic mechanisms. *Nat. Rev. Neurol.* **2016**, *12* (3), 135−149.

https://doi.org/10.1021/acsnano.3c11049
ACS Nano XXXX, XXX, XXX−XXX